Journal of Medicinal Chemistry

pubs.acs.org/jmc

Article

Discovery of Covalent Inhibitors Targeting the Transcriptional Enhanced Associate Domain Central Pocket

Hacer Karatas, Mohammad Akbarzadeh, Hélène Adihou, Gernot Hahne, Ajaybabu V. Pobbati, Elizabeth Yihui Ng, Stéphanie M. Guéret, Sonja Sievers, Axel Pahl, Malte Metz, Sarah Zinken, Lara Dötsch, Christine Nowak, Sasikala Thavam, Alexandra Friese, CongBao Kang, Wanjin Hong, and Herbert Waldmann*

Cite This: *J. Med. Chem.* 2020, 63, 11972−11989

Read Online

ACCESS | Metrics & More | Article Recommendations | Supporting Information

ABSTRACT: Transcriptional enhanced associate domain (TEAD) transcription factors together with coactivators and corepressors modulate the expression of genes that regulate fundamental processes, such as organogenesis and cell growth, and elevated TEAD activity is associated with tumorigenesis. Hence, novel modulators of TEAD and methods for their identification are in high demand. We describe the development of a new "thiol conjugation assay" for identification of novel small molecules that bind to the TEAD central pocket. The assay monitors prevention of covalent binding of a fluorescence turn-on probe to a cysteine in the central pocket by small molecules. Screening of a collection of compounds revealed kojic acid analogues as TEAD inhibitors, which covalently target the cysteine in the central pocket, block the interaction with coactivator yes-associated protein with nanomolar apparent IC_{50} values, and reduce TEAD target gene expression. This methodology promises to enable new medicinal chemistry programs aimed at the modulation of TEAD activity.

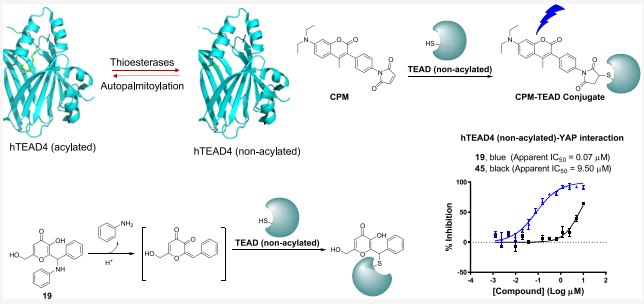

INTRODUCTION

Transcriptional enhanced associate domain (TEAD) transcription factors play significant roles during development, tissue regeneration, cell growth, and migration and in human disease progression.[1−4] Elevated TEAD expression has been observed in solid tumors such as prostate,[5] lung,[6] colorectal,[7] gastric,[8] and breast cancers.[9] A number of TEAD target genes including cell surface receptor tyrosine kinase Axl,[10] connective tissue growth factor (CTGF),[11,12] apoptosis inhibitor survivin,[13] and tumor marker mesothelin[14] are also frequently associated with tumorigenesis. Therefore, TEAD transcription factors are potential therapeutic targets in cancer therapy.

There are four TEAD homologues (TEAD1−4) in mammalian cells that are expressed in a tissue development stage-specific manner. TEAD1 is involved in cardiogenesis, while TEAD2 is critical for neural development and TEAD4 is necessary for embryo implantation.[15−18] Thus, pharmacological modulation of TEAD activity may enable novel medicinal chemistry approaches both in oncology and regenerative medicine.[19,20] Accordingly, the development of small-molecule and peptidic modulators of the TEAD function has been approached.[1,20−23]

TEAD homologues 1−4 share two highly conserved N- and C-terminal domains. The N-terminal DNA-binding domain forms a homeodomain and the C-terminal transactivation domain adopts a β-sandwich capped with a helix-turn-helix motif (Figure 1A, left panel, cyan).[1] The transactivation domain maintains the interaction with transcriptional comodulators, that is, coactivators yes-associated protein (YAP) (Figure 1A, left panel, pale yellow), transcriptional coactivator with PDZ-binding motif (TAZ), vestigial-like (Vgll) family proteins, and corepressor Vgll4 (Figure S1).[24,25]

TEADs contain a large hydrophobic central pocket within the globular β-sandwich to which the cofactors bind. The pocket embodies a conserved cysteine residue that can be acylated with palmitic or myristic acid (Figure 1A).[26−28] Recent studies suggest that TEAD acylation is dynamically regulated by auto-palmitoylation and depalmitoylases,[26,29] pointing to a possibility of targeting the TEAD central pocket via the nonacylated form (Figure S2).

Indeed, the nonacylated hydrophobic central pocket can be targeted by small molecules that bind to the lipidation site

Received: July 22, 2020
Published: September 10, 2020

https://dx.doi.org/10.1021/acs.jmedchem.0c01275
J. Med. Chem. 2020, 63, 11972−11989

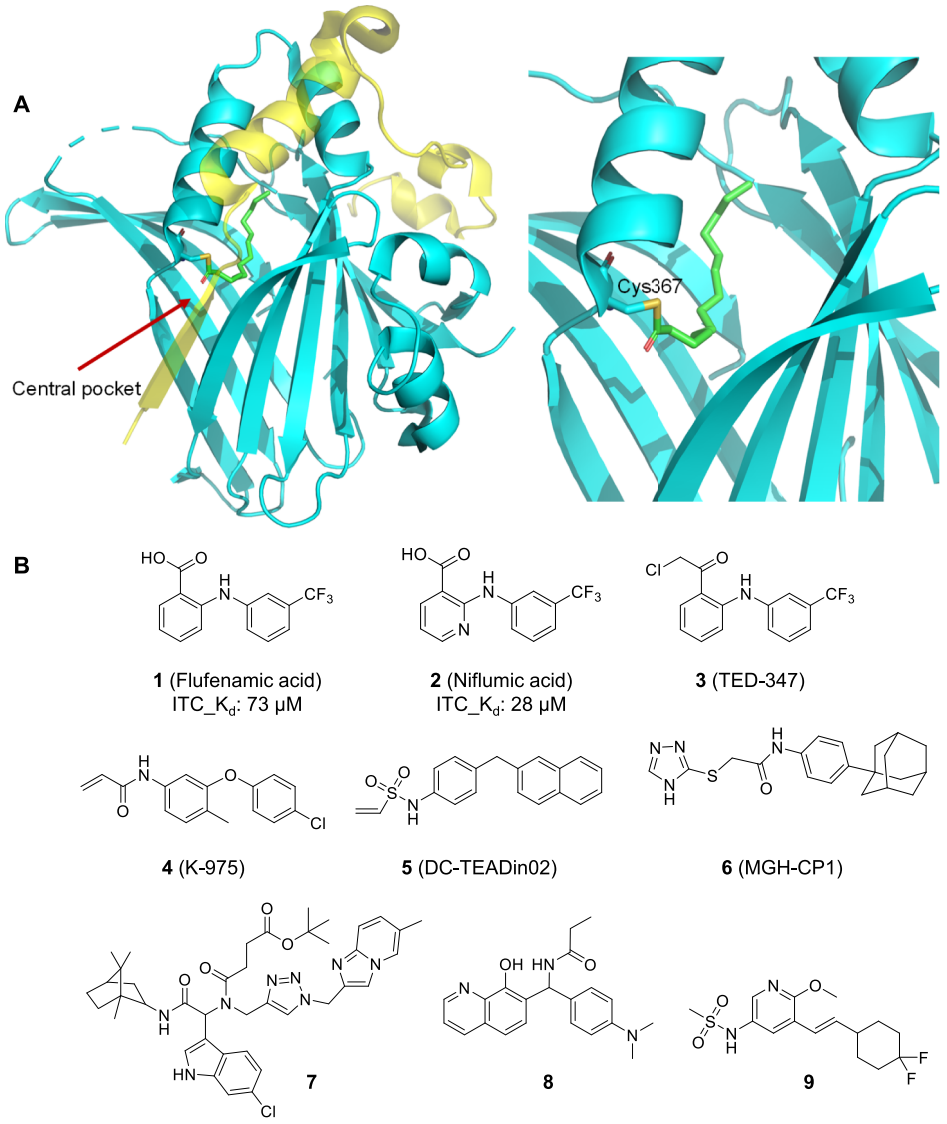

Figure 1. hTEAD4 transactivation domain. (A) Structure of the TEAD transactivation domain (cyan) and the acylated cysteine residue in the central pocket (PDB ID: 5OAQ). Cofactor YAP (PDB ID: 3KYS) is shown (pale yellow). The right panel is zoomed into the acylated cysteine residue (Cys367). (B) Small molecules that bind the TEAD central pocket.

(Figure 1B). Nonsteroidal anti-inflammatory drugs flufenamic acid (**1**, K_d = 73 μM) and niflumic acid (**2**, K_d = 28 μM) bind to the TEAD central pocket and inhibit expression of TEAD−YAP target genes and growth of cancer cell lines.[30] Furthermore, a chloromethylketone analogue of flufenamic acid (**3**, **TED-347**) was developed as a covalent TEAD inhibitor that can allosterically inhibit the TEAD−YAP interaction (K_i = 10.4 μM).[31] Another covalent TEAD inhibitor (**4**, **K-975**) showed efficacy in human malignant pleural mesothelioma xenograft models.[32] More recently, a vinylsulfonamide derivative (**5**, **DC-TEADin02**) was developed via structure-based virtual screening and was shown to covalently bind to TEAD in cells transfected with Flag-TEAD4.[33] Triazole **6** efficiently inhibits TEAD palmitoylation in intestinal epithelium in vivo,[34] and compound **7** was identified via screening a DNA-ecoded library with indole-focused Ugi-peptidomimetics.[35] Furthermore, the hydroxyquinoline analogue **8** was reported to bind the central pocket, however, it activates the TEAD function.[36] A recently identified TEAD palmitoylation inhibitor (**9**) mimics the palmitate-binding mode, activates TEAD to act as a transcriptional repressor independent from YAP, and inhibits tumor growth in a xenograft model.[37] Overall, the number and diversity of small molecules that target the TEAD central pocket has been growing, and any methodology that will aid the development of novel TEAD modulators will be invaluable.

We describe the development of a new methodology for the identification of novel small-molecule inhibitors binding to the TEAD central pocket. By means of a newly developed "thiol conjugation assay" we identified kojic acid derivatives that covalently target the palmitoylatable cysteine in the TEAD central pocket and inhibit the TEAD−YAP interaction with nanomolar apparent IC_{50} values. By means of a representative analogue, we have shown the TEAD engagement in cell lysates and the inhibition of the expression of the TEAD target gene ANKRD1. The novel methodology in general promises to enable new medicinal chemistry programs aimed at the discovery of covalent or noncovalent TEAD inhibitor classes.

https://dx.doi.org/10.1021/acs.jmedchem.0c01275
J. Med. Chem. 2020, 63, 11972−11989

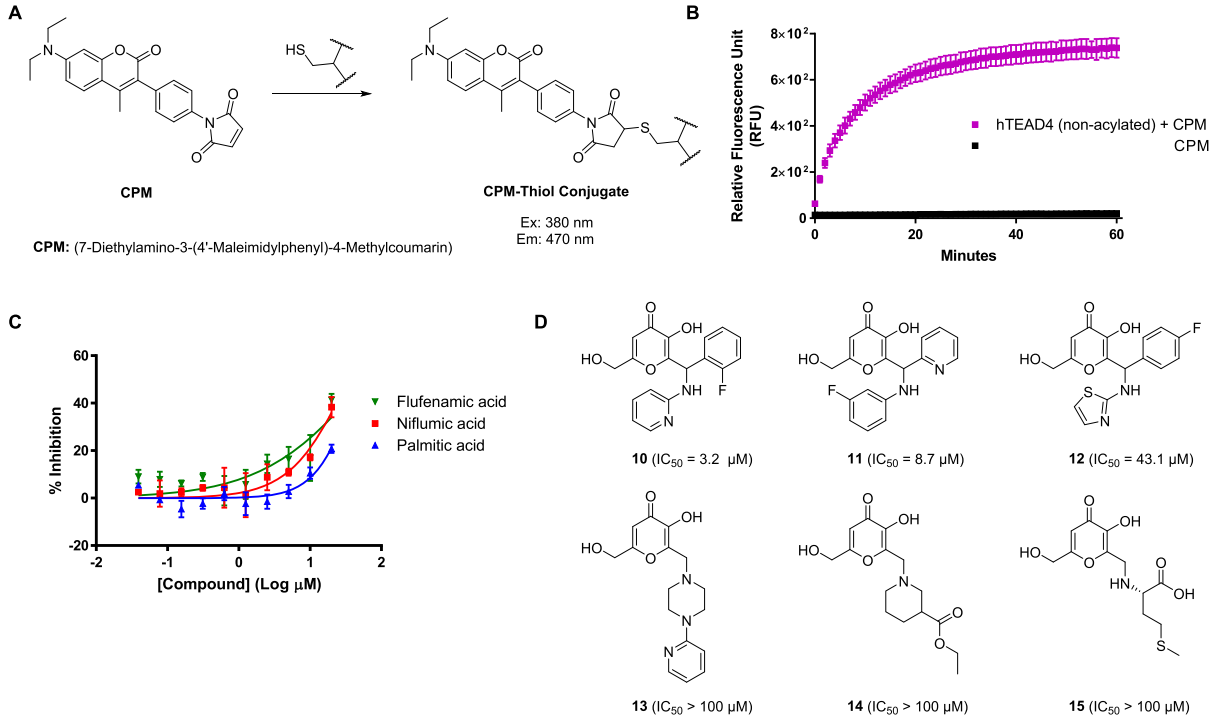

Figure 2. Targeting the central pocket with small-molecule inhibitors. (A) Thiol conjugation assay principle. The free cysteine residue in the TEAD central pocket reacts with CPM yielding a fluorescence signal. (B) Kinetic measurement of hTEAD4 (nonacylated) treatment with CPM (purple square) yields a fluorescence signal, while CPM alone (black square) has only a minimal signal. (C) Competitive inhibition of hTEAD4 (nonacylated) CPM with known noncovalent central pocket binders. (D) Selected screening hits (**10**−**12**) and inactive analogues (**13**−**15**) with similar structures.

Scheme 1. Synthesis of Kojic Acid Analogues[a]

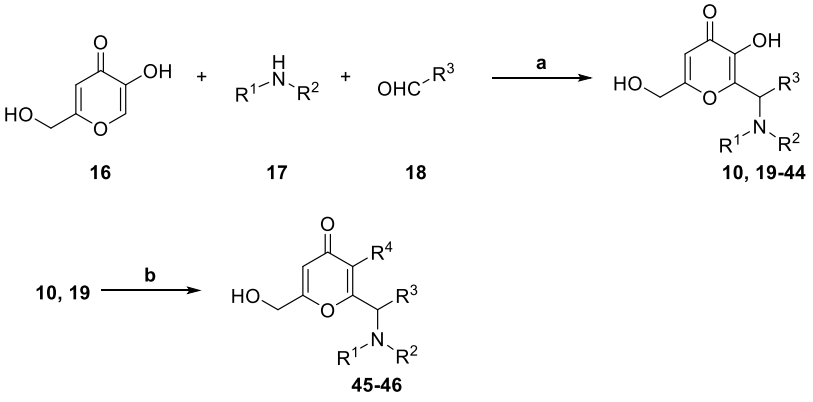

[a]Reagents and conditions: (a) EtOH, rt, 2−20 days. (b) MeI, K_2CO_3, DMF, 24 h, rt.

RESULTS AND DISCUSSION

Development of a "Thiol Conjugation Assay". In order to develop a robust, homogeneous, and rapid binding assay for the TEAD central pocket, we utilized the thiol-reactive profluorescent probe, *N*-(4-(7-diethylamino-4-methylcoumarin-3-yl)phenyl)maleimide (CPM) that has been used for site-specific protein labeling, thermal stability analysis of membrane proteins, and assaying *N*-acyltransferase activity.[38−42] The fluorescence in CPM is quenched because of the maleimide substitution on the phenyl group that modulates the resonance between the coumarin carbonyl and 7-amino groups. However, upon reaction with a thiol, CPM fluorescence increases strongly (Figure 2A).[41] We hypothesized that the reaction of a free cysteine residue in the TEAD central pocket would yield a fluorescence signal and that small molecules binding to the TEAD central pocket with appreciable potency would prevent covalent labeling of the cysteine by CPM.

For assay development, hTEAD4 was delipidated with hydroxylamine to cleave the covalent thioester bond between the fatty acid and the cysteine (Cys367 for hTEAD4, Figure 1A right panel). Delipidation was monitored and confirmed with whole-protein electron spray ionization (ESI)−mass spectrometry (MS) (Figure S3). Through expression, a mixture of the three recombinant[28] nonacylated hTEAD4 (MW: 26,495) and hTEAD4 covalently bound to either myristic acid (C14-fatty acid, MW: 26,705) or palmitic acid (C16-fatty acid, MW: 26,733) (Figure S3A) was converted to a homogeneous nonacylated hTEAD4 protein (MW: 26,495) (Figure S3B).

https://dx.doi.org/10.1021/acs.jmedchem.0c01275
J. Med. Chem. 2020, 63, 11972−11989

Addition of the nonacylated hTEAD4 to 1 equivalent CPM yielded a significant increase in the fluorescence signal, which reached a plateau in 30−40 min (Figure 2B). Analysis of the reaction mixture with ESI−MS indicated that two cysteine residues might have been labeled with CPM (Figure S4A). Subsequent tandem MS (MS−MS) analysis showed that Cys367 and Cys330, both of which are located in the hTEAD4 central pocket, were covalently modified with CPM (Figures S4B and S5). These findings suggested that monitoring of CPM binding to the TEAD central pocket and its prevention by small molecules could be used to identify novel TEAD central pocket-targeting inhibitors.

For validation, we investigated inhibition of CPM binding and fluorescence decrease by the known TEAD central pocket binders, flufenamic acid (**1**), niflumic acid (**2**), palmitic acid, and the covalent inhibitor **3** (TED-347). As shown in Figure 2C for noncovalent binders and in Figure S6 for TED-347, these compounds inhibited the signal increase in a dose-dependent manner. To our best knowledge, this is the first example that CPM is used for a binding assay. Because a cysteine thiol is necessary in the reaction with CPM, we termed this novel assay "Thiol Conjugation Assay".

Discovery of Small-Molecule Inhibitors of the TEAD Central Pocket. Investigation of a collection of 14,000 compounds using the newly established thiol conjugation assay identified 329 compounds, which showed >50% inhibition at a concentration of 12.5 μM (2.3% primary hit rate). Kojic acid analogues **10**−**12** (Figure 2D) were among the most potent hits. Analogues **13**−**15** lacking aryl substituents on the methyl amine, however, were inactive (Figure 2D) such that for initial structure−activity relationship (SAR) investigations, a phenyl group at both R^1 and R^3 positions was retained (Scheme 1). Compounds **19**−**44** were synthesized using a one-pot Betti reaction[43] starting from kojic acid (**16**), amines **17**, and aldehydes **18** (Scheme 1). In addition, the 2-hydroxyl group in compounds **19** and **10** was methylated to yield compounds **45** and **46**, respectively.

Direct binding of compounds **19**−**46** to the TEAD central pocket was monitored by means of a fluorescence polarization (FP)-based competitive binding assay employing a fluorescein isothiocyanate (FITC)-labeled palmitate tracer (Scheme S1), which bound with K_d = 28 nM to nonacylated hTEAD4 (Figure S7A). The FP assay was validated employing the previously reported competitive inhibitor niflumic acid (**2**) as a positive control (Figure S7B).

IC_{50} values obtained from the thiol conjugation assay and the FP-based competitive binding assay are shown in Table 1. Not surprisingly, because of the different assay principles (i.e., competition with the covalent cysteine binder CPM *vs* competition with noncovalent binder FITC-palmitate) and protein concentrations, the IC_{50} values obtained from the FP and thiol conjugation assays differ for all kojic acid analogues, consistently 5−10-fold.

Initial SAR investigations focused on modifications of amine substituents R^1 and R^2 (Table 1). Replacement of the phenyl group in **19** by an isopropyl group (**20**) led to a sevenfold increase in IC_{50} values for both assays. Although a benzyl group (**21**) was slightly (twofold) less favorable than the phenyl group (**19**), the introduction of the constrained bis-benzyl moiety in **22** lowered the affinity nearly fivefold. A fluorine group at the meta-position of R^1 (**23**) did not influence TEAD binding, and introduction of an electron-deficient 2-pyridine ring (**24**) gave a similar IC_{50} value as for a

Table 1. SAR Studies of the Kojic Acid Analogues

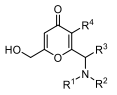

Compound ID	R^1	R^2	R^3	R^4	Apparent IC_{50} (μM)	
					Thiol Conjugation	Fluorescence Polarization
19		-H		-OH	2.3 ± 0.3	0.2 ± 0.04
20		-H		-OH	16.8 ± 0.9	1.5 ± 0.2
21		-H		-OH	4.0 ± 0.6	0.4 ± 0.03
22				-OH	13.2 ± 2.7	0.9 ± 0.3
23		-H		-OH	1.5 ± 0.4	0.2 ± 0.05
24		-H		-OH	3.1 ± 0.6	0.3 ± 0.03
25		-H		-OH	2.4 ± 0.3	0.3 ± 0.08
26		-H		-OH	> 100	13.4 ± 3.3
27		-H		-OH	53.4 ± 11.5	5.6 ± 0.9
28		-H		-OH	> 100	6.4 ± 0.9
29		-H		-OH	1.7 ± 0.2	0.3 ± 0.09
30		-H		-OH	> 100	22.6 ± 2.8
31		-H		-OH	> 100	38.1 ± 8.4
32		-H		-OH	> 100	36.4 ± 11.9
33		-H		-OH	1.5 ± 0.2	0.3 ± 0.1
34		-H		-OH	1.3 ± 0.3	0.2 ± 0.03
35		-H		-OH	1.9 ± 0.2	0.3 ± 0.01
36		-H		-OH	1.2 ± 0.4	0.2 ± 0.06
37		-H		-OH	1.0 ± 0.3	0.2 ± 0.04
38		-H		-OH	1.1 ± 0.3	0.2 ± 0.05
39		-H		-OH	0.7 ± 0.1	0.1 ± 0.03
40		-H		-OH	18.9 ± 6.2	0.5 ± 0.1
41		-H		-OH	9.2 ± 2.1	1.1 ± 0.2
42		-H		-OH	3.7 ± 0.1	0.4 ± 0.06
10		-H		-OH	3.2 ± 0.6	0.3 ± 0.03
43		-H		-OH	> 100	16.0 ± 2.6
44		-H		-OH	> 100	14.7 ± 3.9
45		-H		$-OCH_3$	> 100	41.6 ± 7.3
46		-H		$-OCH_3$	> 100	49.9 ± 4.8
2					41.9 ± 10.5	5.9 ± 1.1
3 (TED-347)					0.8 ± 0.4	14.1 ± 4.0

https://dx.doi.org/10.1021/acs.jmedchem.0c01275
J. Med. Chem. 2020, 63, 11972−11989

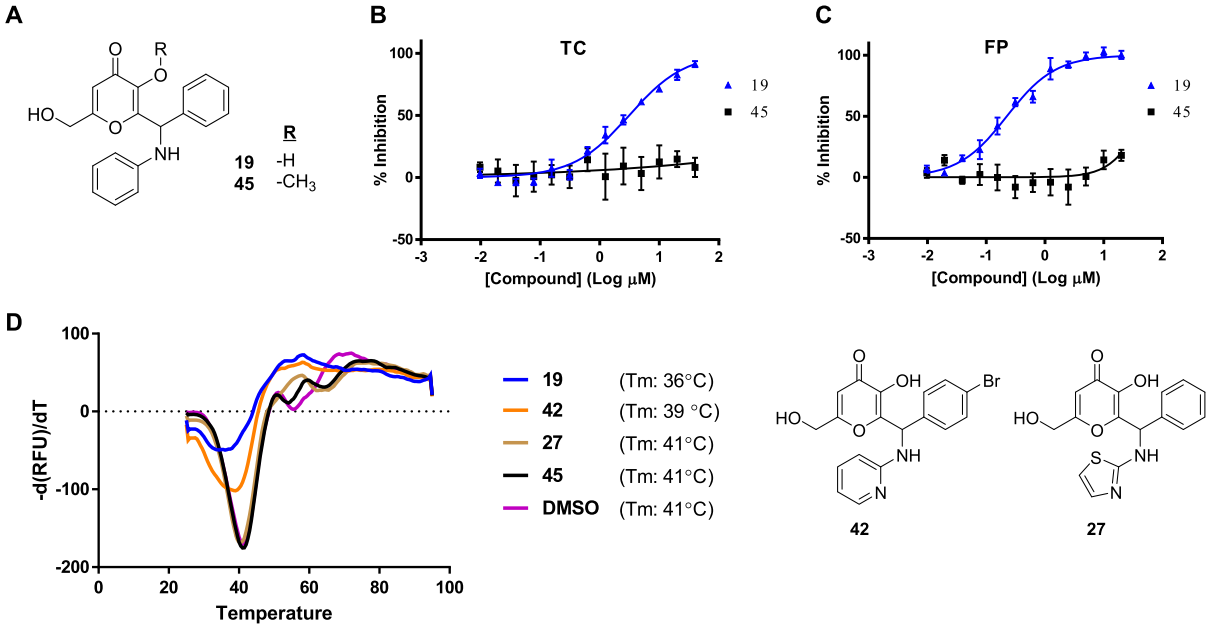

Figure 3. Target engagement studies with compound **19** and its inactive analogue **45** in cell-free systems. (A) Structures of the compounds **19** and **45**. Representative inhibition curves in the (B) thiol conjugation assay and (C) FP-based competitive binding assay. (D) Differential scanning fluorimetry measurements of hTEAD4 (nonacylated) with selected derivatives.

phenyl group (**19**). Substitution of the 2-pyridine ring (**25**) with a methyl group on the 5-position also did not alter the binding. However, the introduction of 2-pyrimidine- (**26**), 2-thiazole- (**27**), and 2-benzimidazole (**28**) groups resulted in more than 20-fold increase in the IC_{50} values. Equipment of the phenyl ring at R^1 with an electron-withdrawing 4-carboxamide (**29**) did not influence the affinity.

Replacement of the benzylic phenyl group at the R^3 position with an aliphatic cyclohexyl (**30**) or isopropyl group (**31**) or with a hydrogen (**32**) dramatically (100-fold) reduced TEAD binding in the thiol conjugation assay showing the importance of an aromatic residue at the R^3 position. Introduction of an electron-withdrawing carboxamide substituent at the para-position (**33**) slightly (twofold) improved binding. Hydrophobic substituents at the para-position (**34**−**38**) did not change binding significantly, and similarly, introduction of a fluorine group (**39**) at the ortho-position was tolerated. Replacement of the phenyl ring with an electron-deficient 2-pyridine group (**40**), however, lowered the inhibitory activities by 2−3-fold in the FP assay.

Additional analogues with 2-pyridine residues at R^1 and R^3 (**41**−**44**), in particular, the combination of two 2-pyridines at both R^1 and R^3 positions (**43**), lowered the affinity significantly.

The importance of a 2-OH group at the R^4 position was proven by investigation of compounds **45** and **46**, that is, the 2-OMe analogues of compounds **19** and **10**, respectively. Both compounds were inactive in the thiol conjugation assay and had >200-fold lower affinity in the FP assay, showing the critical influence of the 2-OH group for TEAD binding (Figure 3A−C).

We additionally confirmed the TEAD binding of selected analogues (**19**, **27**, **42**, and **45**) using differential scanning fluorimetry (Figure 3D). Compound **19** lowered the melting point (T_m) of nonacylated hTEAD4 by 5 °C, and its 2-pyrido (R^1), 4-bromo (R^3) analogue (**42**) induced a smaller T_m shift (−2 °C) aligning with the binding experiments (Table 1). Consistent with the competitive binding experiments, compounds **27** and **45** did not induce any change in the T_m of nonacylated hTEAD4.

Covalent Binding to the TEAD Central Pocket. In light of the observation that a nonmodified, acidic 2-OH group in kojic acid (pK_a = 7.9)[44] is required for activity, we reasoned that the compounds of type **19** might undergo a retro-Mannich reaction to yield a Michael acceptor, which then could covalently react with Cys367 in nonacylated hTEAD4 (Figure 4A). In agreement with this hypothesis, methylation of the 2-OH group (**45** and **46**) led to compounds inactive in the thiol conjugation assay (Figure 3B, Table 1). Indeed, treatment of nonacylated hTEAD4 with 8 equiv of compound **19** or **45** and subsequent analysis of the mixture with whole-protein ESI−MS spectrometry revealed that—consistent with our hypothesis—modification of the protein (+230 Da) was observed upon incubation with **19** (Figure 4A−B), while modification of TEAD was not observed upon coincubation with **45** (Figure 4C).

The hypothesis that compound **19** specifically targets Cys367 that is lipidated under physiological conditions was further strengthened by the observation that incubation of **19** with acylated (i.e., not treated with hydroxylamine) hTEAD4 did not result in the formation of an acylated hTEAD4-**19** adduct (Figures 4D and S3A).

In addition, mutants of mouse TEAD4 (mTEAD4) in which the reactive cysteine was replaced with alanine or serine and that should not react with compound **19** were investigated in the thiol conjugation assay. As shown in Figure 4E, compound **19** cannot inhibit an increase in the fluorescence signal when the Ser or Ala mutant of mTEAD4 is used. Collectively, these observations show that kojic acid analogue **19** covalently and specifically binds nonacylated TEAD4.

To confirm the covalent reaction between compound **19** and nonacylated hTEAD4, thiol conjugation and FP assays were used to determine the time-dependent inhibition (TDI) of hTEAD4. Compound **19** showed a low-micromolar

https://dx.doi.org/10.1021/acs.jmedchem.0c01275
J. Med. Chem. 2020, 63, 11972−11989

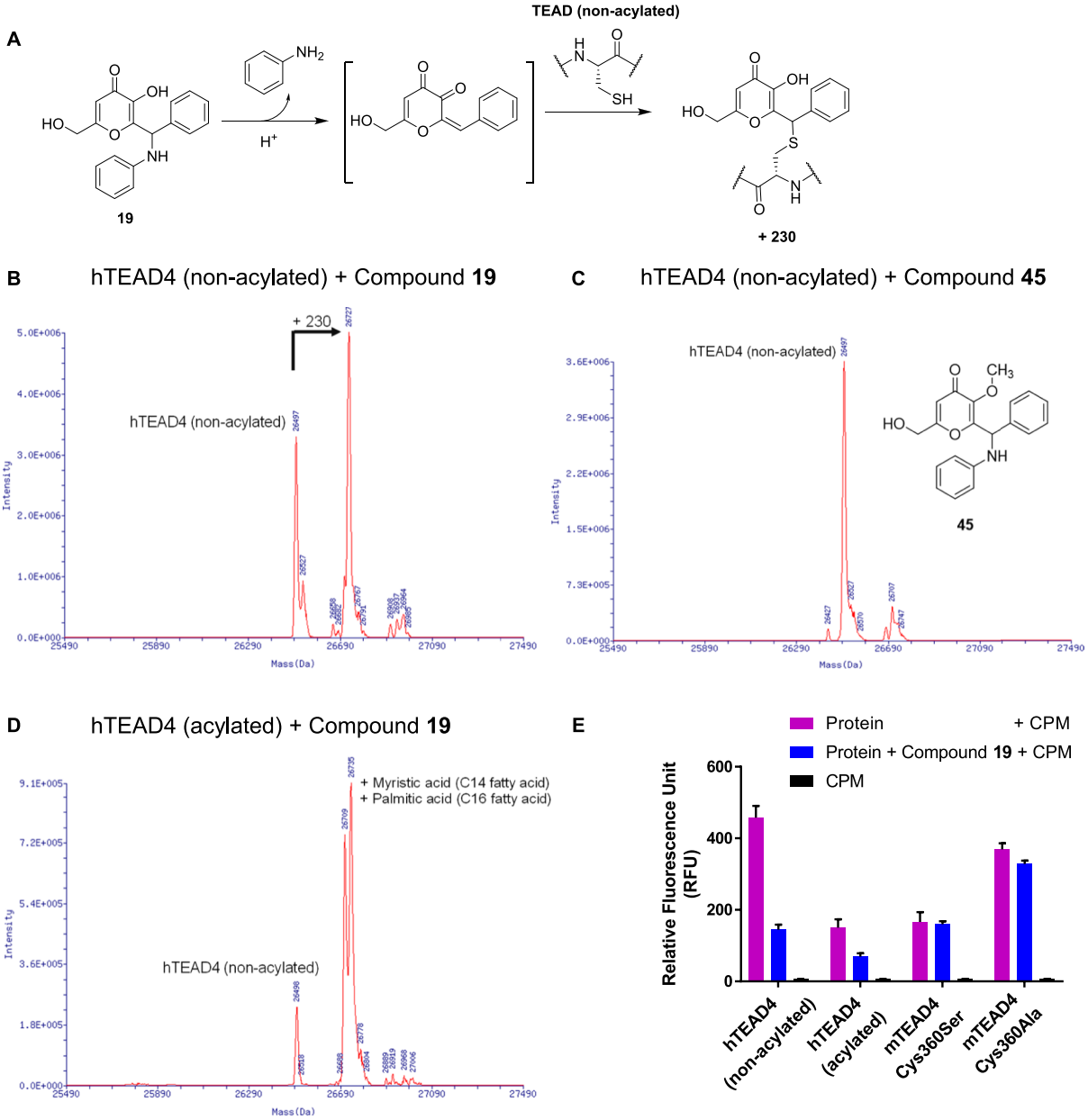

Figure 4. Mechanism of action studies with kojic acid analogues. (A) Hypothesized mechanism of action of compound **19**. Whole-protein ESI−MS analysis of hTEAD4 (nonacylated) treatment with kojic acid analogue (B) compound **19** and (C) compound **45**. Compound **19** is a covalent binder for nonacylated hTEAD4, and the −OH group at the second position is required for the predicted reaction with a thiol group. The −OMe analogue (**45**) is not a covalent TEAD binder. (D) Whole-protein ESI−MS analysis of hTEAD4 (acylated) incubation with **19**. No protein adduct with compound **19** was observed when Cys367 in hTEAD4 is lipidated. (E) Comparison of thiol conjugation inhibition with 10 μM compound **19** in the presence of hTEAD4 (nonacylated), hTEAD4 (acylated), or Cys to Ala/Ser mutants of mTEAD4. When the cysteine residue is replaced with alanine or serine, compound **19** cannot inhibit the thiol conjugation.

inhibition constant (K_i = 2.6 μM), which describes the potency of reversible binding between the compound and the protein before the covalent bond formation (Figure S8A,B). Compound **19** inhibited nonacylated hTEAD4 with k_{inact}/K_i = 8.3 μM in the thiol conjugation assay and with k_{inact}/K_i = 4.0 μM in the FP assay (Figure S8C,D).

Investigation of the specificity of compound **19** for binding to TEAD homologues by means of the thiol conjugation assay showed that **19** inhibits hTEAD1−4 with similar low-micromolar IC_{50} values (2.6−6.9 μM, Figure S9) consistent with the high homology (72.0−87.9%)[1] of the transactivation binding domains of TEAD1−4.

Binding Mode Analysis. To get insight into the binding mode and binding site of the new covalent inhibitors, $^{1}H-^{15}N$ HSQC spectra of mTEAD4 in the absence and presence of compound **19** or **45** were recorded, and signals were assigned based on the corresponding analysis[45] of the transactivation domain of mTEAD4. Compound **19** induced line broadening of several residues (Figure S10A), including Phe386 (F386) and Phe408 (F408). These amino acids are in close proximity to the palmitoylation site. Conversely, the negative control **45** did not induce a significant change compared to the dimethyl sulfoxide (DMSO) control (Figure S10B). These findings

https://dx.doi.org/10.1021/acs.jmedchem.0c01275
J. Med. Chem. 2020, 63, 11972−11989

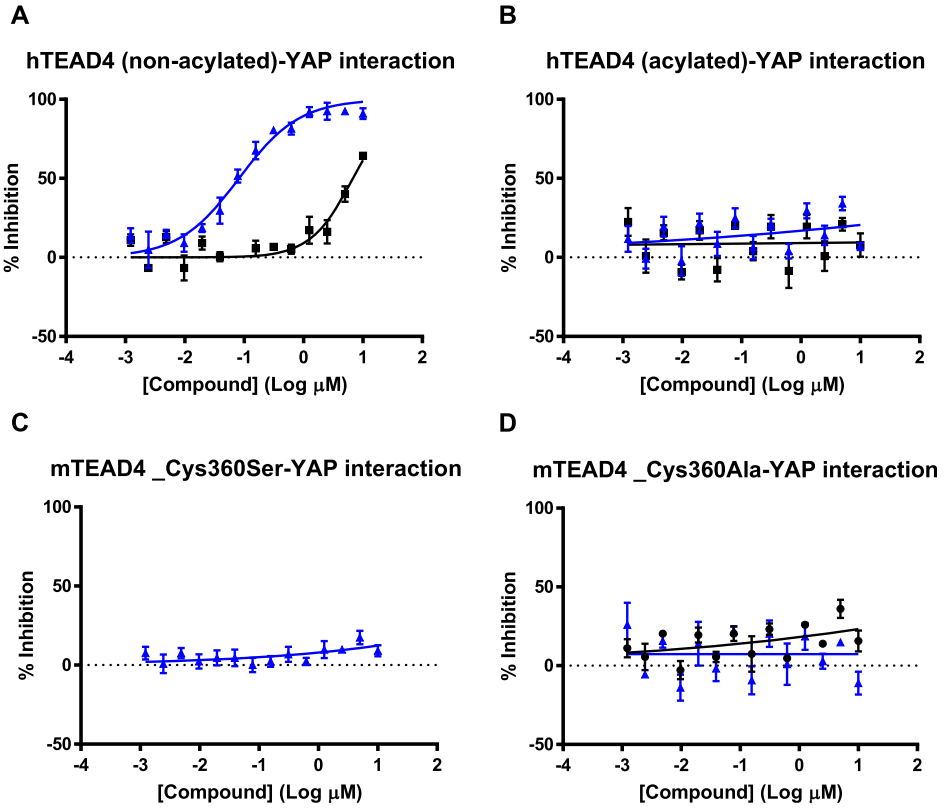

Figure 5. Inhibition of TEAD−YAP interaction as determined with an FP-based competitive binding assay using FITC-labeled $hYAP^{50-100}$. Compound **19** (blue triangle) and compound **45** (black square) were tested. (A) Compound **19** can prevent YAP interaction with hTEAD4 (nonacylated) but not with (B) hTEAD4 (acylated), mTEAD4 with (C) Cys360Ser, or (D) Cys360Ala mutation.

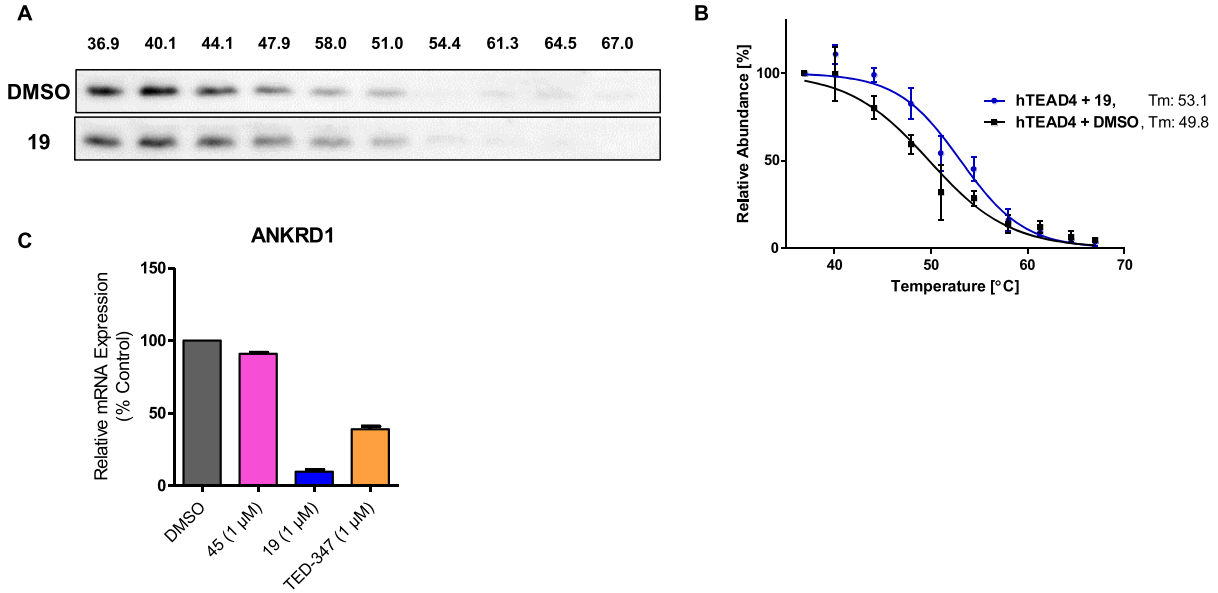

Figure 6. TEAD inhibitory activity of **19** in a cellular environment. (A,B) Target engagement in HCT116 cell lysates. (A) Representative immunoblots of hTEAD4 treated with a vehicle control (DMSO) or compound **19**. (B) CETSA melting curves of hTEAD4 treated with a vehicle control (DMSO) or compound **19**. (C) Inhibition of the TEAD target gene ANKRD1 expression by compound **19** in comparison with the control compounds **45** and TED-347.

support the biochemical data suggesting that compound **19** binds to the central pocket in TEAD.

Covalent TEAD Binders Inhibit the TEAD−YAP Interaction. The chloromethyl ketone flufenamic acid analogue (**3**, TED-347) that binds the TEAD central pocket covalently allosterically inhibits TEAD and YAP interaction and consequently YAP-mediated target gene expression.[31] In order to determine whether the new inhibitor class can also disrupt this protein−protein interaction, an FP assay that monitors the binding of the fluorescently labeled YAP peptide

https://dx.doi.org/10.1021/acs.jmedchem.0c01275
J. Med. Chem. 2020, 63, 11972−11989

to nonacylated hTEAD4 was used. Preincubation with compound **19** for 10 min potently inhibited the interaction of nonacylated hTEAD4 with human YAP^{50-100} with an IC_{50} value of 70 nM. In contrast and in agreement with the covalent inhibition mechanism proposed above, the OMe analogue **45** had >100-fold lower activity (IC_{50} = 9.5 μM) (Figure 5A) and covalent inhibitor **19** did not inhibit the interaction of YAP with acylated hTEAD4 and mTEAD4 with Cys360Ser or Cys360Ala mutations (Figure 5B–D) (saturation binding curves of FITC-YAP^{50-100} with the TEAD4 proteins are shown in Figure S11A–D). Overall, these results are in accordance with previous findings[31] for covalent allosteric inhibition of TEAD and show that the covalent and potent TEAD central pocket-binding small molecules identified here can block the TEAD–YAP interaction efficiently.

TEAD Engagement in a Cellular Environment. Target engagement in HCT116 cell lysates was proven by means of a cellular thermal shift assay (CETSA). Treatment of the lysates with compound **19** for 10 min increased the melting temperature of hTEAD4 from 49.8 to 53.1 °C (ΔT_m = 3.3 °C), providing evidence for the interaction with hTEAD4 in a biologically relevant environment (Figure 6A,B).

TEADs, together with the coactivators (e.g., YAP), regulate the expression of genes involved in critical processes such as cardiogenesis, cell growth, and migration.[2] Small molecules that bind the TEAD central pocket have been shown to modulate the TEAD transcriptional activity, such as inhibition of the expression of well-established TEAD target genes (i.e., ANKRD1, CTGF, and CYR61).[34,37] To evaluate the influence of kojic acid analogues on TEAD transcriptional activity, HEK293 cells were incubated with compound **19**, negative control **45**, or TED-347. Treatment with compound **19** for 6 h resulted in 90% reduction of the mRNA level of the TEAD target gene ANKRD1 compared to the DMSO control, while compound **45** had only a minimal effect at the same concentration, further supporting the on-target activity of the kojic acid analogues (Figure 6C).

CONCLUSIONS

We have developed a new "thiol conjugation assay" that enables the systematic identification of small-molecule inhibitors of the TEAD central pocket. By means of this assay, kojic acid analogues were identified as a new class of TEAD inhibitors. Our data show that these inhibitors covalently bind to the Cys residue in the TEAD central pocket that is S-acylated under physiological conditions. The representative kojic acid analogue **19** inhibited the interaction of YAP with nonacylated hTEAD4 but not with the corresponding acylated protein and mutants, in which the Cys had been replaced by a serine or an alanine. Furthermore, CETSA in lysate provided evidence for compound **19** interacting with hTEAD4 in a biologically relevant medium. Consistent with the binding experiments, kojic acid analogue **19** inhibited TEAD target gene expression. Taken together, we have established a novel methodology that could be a guide for the development of novel classes of TEAD inhibitors interacting with the protein covalently or noncovalently.

EXPERIMENTAL SECTION

Plasmids. hTEAD4 plasmid was isolated from the cDNA clone of hTEAD4 (Dharmacon, clone ID: 3913870). The plasmid with mTEAD4 with a Cys360Ala mutant was obtained through site-directed mutagenesis using an mTEAD4 wild-type template (Dharmacon, clone ID: 40142595). All plasmids were verified by DNA sequencing.

Cloning, Expression, and Purification of Recombinant Proteins. Sequences of the proteins used in the study are shown in Table S1.

N-His hTEAD4. The plasmid of N-terminal His_6-tagged $hTEAD4^{217-434}$ was subcloned into a pOPIN-neo vector, which was used to transform *Escherichia coli* BL21-CodonPlus (DE3)-RIPL (Agilent, 230280). The transformed cells were grown in the TB medium supplemented with 0.01% α-lactose monohydrate, 2 mM $MgSO_4$, 100 μg/mL ampicillin, and 50 μg/mL chloramphenicol at 37 °C for 4 h. Then, the temperature was reduced to 25 °C and the culture was incubated for a further 20–24 h. The cells were harvested, and the pellets were taken in a lysis buffer containing 50 mM HEPES, 300 mM NaCl, 20 mM imidazole, and 1 mM TCEP, pH 8 and lysed by sonication, followed by ultracentrifugation. Then, the cleared lysate was loaded onto the ÄktaXpress (GE Healthcare) for affinity purification (His trap FF, GE Healthcare) which was followed by size exclusion chromatography (SD75 26/60, GE Healthcare) using 20 mM HEPES, 100 mM NaCl, 1 mM TCEP, 2 mM $MgCl_2$, and 5% glycerol, pH 8. The purified protein was concentrated using Amicon Ultra Centrifugal Filters, 10K (Merck), and aliquots were snap-frozen and stored at −80 °C.

N-His mTEAD4_Cys360Ser. A method provided earlier was used for the protein expression using 1 mM IPTG.[45] The harvested cell pellets were lysed, and the protein was purified as described above for N-His hTEAD4.

N-His-MBP mTEAD4_Cys360Ala. cDNA of N-terminal His_6- and MBP-tagged $mTEAD4^{209-427}$ with Cys360Ala mutation was used to transform *E. coli* BL21-CodonPlus (DE3)-RIPL (Agilent, 230280). The protein was expressed, and the collected pellets were lysed as described for N-His hTEAD4 above. The cleared lysate was loaded onto the ÄktaXpress (GE Healthcare) for affinity purification (His trap FF, GE Healthcare) which was followed by size exclusion chromatography (SD200 16/60, GE Healthcare) using 25 mM HEPES, 150 mM NaCl, and 1 mM TCEP, pH 7.2. The purified protein was concentrated using Amicon Ultra Centrifugal Filters, 50K (Merck), and aliquots were snap-frozen and stored at −80 °C. The storage buffer was exchanged with pH 8 Tris-HCl (20 mM), NaCl (100 mM), and $MgCl_2$ (2 mM) using Amicon Ultra Centrifugal Filters (10K) for the binding studies.

N-His-GST hTEAD1. The plasmid of N-terminal His_6-tagged GST-$hTEAD1^{209-426}$ was subcloned into a pOPIN-neo vector, which was used to transform *E. coli* BL21-CodonPlus (DE3)-RIPL (Agilent, 230280). The transformed cells were grown in TB medium supplemented with 2 mM $MgSO_4$, 100 μg/mL ampicillin, and 50 μg/mL chloramphenicol at 37 °C until the optical density reached 0.6. Then, the temperature was reduced to 18 °C and the culture was incubated for a further 16 h. The cells were harvested, and the pellets were taken in a lysis buffer containing 50 mM HEPES, 300 mM NaCl, 20 mM imidazole, and 1 mM TCEP, pH 8 and lysed by sonication, followed by ultracentrifugation. Then, the cleared lysate was loaded onto the ÄktaXpress (GE Healthcare) for affinity purification (His trap FF, GE Healthcare) which was followed by size exclusion chromatography (SD75 26/60, GE Healthcare) using 20 mM HEPES, 100 mM NaCl, 1 mM TCEP, 2 mM $MgCl_2$, and 5% glycerol, pH 8. The purified protein was concentrated using Amicon Ultra Centrifugal Filters, 10K (Merck), and aliquots were snap-frozen and stored at −80 °C.

N-His hTEAD2. The plasmid of N-terminal His_6-tagged $hTEAD4^{217-447}$ was subcloned and the protein was expressed as described above for N-His hTEAD4.

N-His hTEAD3. N-terminal His_6-tagged $hTEAD4^{216-434}$ was expressed using the protocol described for hTEAD4 earlier.[36]

Deacylation (Depalmitoylation) of TEAD. To 500 μL of 105 μM (2.8 mg/mL) recombinant hTEAD4 (acylated) in an Eppendorf tube, 30 μL of freshly prepared 105 mM hydroxyl amine solution was added slowly and the mixture was gently shaken at room temperature for 3–4 h. The deacylation process was monitored with whole-protein ESI–MS. The protein was then purified over two consecutive size

https://dx.doi.org/10.1021/acs.jmedchem.0c01275
J. Med. Chem. 2020, 63, 11972–11989

exclusion columns (i) Amicon, 0.5 mL 10K (Merck) and (ii) Zebaspin, 7K (Thermo Fisher) using Tris (20 mM pH 8), NaCl (100 mM), and $MgCl_2$ (2 mM) as the final storage buffer. Aliquots (5 μL) were snap-frozen and stored at −80 °C.

4 M hydroxylamine solution: 0.46 g (6.67 mmol) of hydroxylamine HCl was dissolved in 0.53 mL of H_2O in a glass vial. Then, 0.33 mL of diethylamine was added dropwise, followed by additional 0.2 diethylamine and 0.63 mL H_2O addition. Freshly prepared 4 M hydroxylamine solution was further diluted to 105 mM with Milli-Q water.

Binding Assays. All the experiments were performed using black, low-volume, round-bottom, nonbinding, 384-well plates (Corning 4514). The plates were imaged using Tecan Spark. Spectramax Paradigm (Molecular Devices) was used for imaging the plates during low-throughput screening. Stock solutions (10 mM) of the compounds in DMSO were used. The K_d of the tracers and the IC_{50} value of the inhibitors were calculated using GraphPad Prism 7 software.

Binding Assays for the TEAD Central Pocket. Thiol Conjugation Assay. To serially diluted solutions of the tested compounds in 5 μL of assay buffer [HEPES (25 mM) and NaCl (150 mM) pH 6.5], freshly prepared 5 μL of 0.45 μM protein solution was added and incubated at room temperature for 10 min, followed by addition of 5 μL of 0.45 μM CPM solution, giving a 15 μL final assay volume, 150 nM protein, and 150 nM CPM. The assay plate was shaken at room temperature for 1 h before measuring the fluorescence (Ex/Em: 380/470 nm). Compound **19** was used as an internal standard to determine 100% inhibition.

Thiol Conjugation Assay for Low-Throughput Screening. A library of 14,000 compounds was screened in 1536-well plates using pH 6.5 MES buffer. To the preincubated solution of nonacylated hTEAD4 (0.15 μM final concentration) and compound solution (12.5 μM final concentration), CPM (0.15 μM final concentration) was added, and the assay plates were incubated at room temperature for 50 min before measuring the fluorescence (Ex/Em: 360/465 nm) using Spectramax Paradigm (Molecular Devices). $Z' = 0.6–0.8$ (10-plates).

Saturation Binding Experiment. To a serially diluted solution of nonacylated hTEAD4 in 12 μL of assay buffer [HEPES (25 mM) and NaCl (150 mM) pH 6.5], 8 μL of 25 nM FITC-palmitate solution was added, giving 20 μL final assay volume with a 10 nM tracer. The assay plate was incubated at room temperature for 1 h before measuring FP (Ex/Em: 485/535 nM).

FP-Based Competitive Inhibition Experiments. To serially diluted solution of the tested compounds in 5 μL assay buffer [HEPES (25 mM) and NaCl (150 mM), pH 6.5 buffer], freshly prepared 5 μL of 0.15 μM protein solution was added and incubated at room temperature for 10 min followed by 5 μL of 30 nM FITC-palmitate solution, giving 15 μL final assay volume, 50 nM protein, and 10 nM tracer. The assay plate was shaken at room temperature for 1 h before measuring the FP (Ex/Em: 485/535 nm).

Binding Assays for TEAD–YAP Interaction. All the TEAD–YAP binding experiments were performed in phosphate-buffered saline (PBS) (pH 7.5).

Saturation Binding Experiments. To a serially diluted solution of the protein in 12 μL PBS, 8 μL of FAM-YAP solution was added, giving 20 μL final assay volume. The assay plate was incubated at room temperature for 1 h before measuring FP (Ex/Em: 485/530 nM). The final FAM concentrations are as follows: hTEAD4 (nonacylated): 2 nM, hTEAD4 (acylated): 2 nM, mTEAD4_Cys360Ser: 10 nM, and mTEAD4_Cys360Ala: 10 nM.

FP-Based Competitive Inhibition Experiments. To serially diluted solution of the tested compounds in 5 μL of PBS, freshly prepared 5 μL of protein solution was added and incubated at room temperature for 10 min followed by addition of 5 μL of FAM-$YAP^{50–100}$ solution. The assay plate was shaken at room temperature for 1 h before measuring the FP (Ex/Em: 485/535 nm). Final protein and FAM concentrations are as follows (FAM/protein): hTEAD4 (nonacylated): 2 nM/5 nM, hTEAD4 (acylated): 3 nM/15 nM, mTEAD4_Cys360Ser: 10 nM/50 nM, and mTEAD4_Cys360Ala: 10 nM/50 nM.

Inhibition Efficiency Experiments. TDI of hTEAD4 (nonacylated) by compound **19** was monitored in FP (central pocket binding) and thiol conjugation assays at 5–7 different concentrations (0.15–40 μM) following 1, 2, 4, and 24 h incubation at 4 °C (mean ± SD; $n = 2$). By fitting the percent of inhibition versus preincubation time at different concentrations, k_{obs} was calculated. Next, k_{obs} was plotted against concentration and was further fitted to a nonlinear regression model to determine the kinetic parameters of covalent inhibition of hTEAD4, where plateau is showing k_{inact} (min^{-1}) and $t_{1/2}$ is K_i (μM).

Differential Scanning Fluorometry. Nonacylated hTEAD4 (20 μM) was incubated in the absence or presence of inhibitors (80 μM) at 25 °C for 10 min. Then, SYPRO orange (Sigma-Aldrich) at a final concentration of 5× was added and the mixture was heated at a ramp rate of 1 °C/min in a qPCR machine (Applied Biosystems). The derivative of the SYPRO orange fluorescent intensity is plotted as a function of temperature.

Whole-Protein ESI–MS. The protein solution (1 μL 5 μM) was injected to UPLC-MS (ThermoScientific_UltiMate 3000 LC coupled to a Velos Pro MS) through a desalting column (MassPREP Online desalting, 2.1 × 10 mm). For reactions, 1 μM of the protein was incubated at room temperature for 1 h with 8 equiv of the compound in HEPES (25 mM) and NaCl (150 mM) pH 6.5 buffer. Then, the mixture was centrifuged before injecting 5 μL. The deconvolution of m/z values was performed using Promass Xcalibur software.

Tandem MS Experiments. *Nonacylated hTEAD4-CPM Reaction.* To 5 μL of assay buffer [HEPES (25 mM) and NaCl (150 mM) pH 6.5], 5 μL of 0.6 μM nonacylated hTEAD4 and 5 μL of 0.6 μM CPM solution were added and incubated at room temperature for 1 h in a 384-well plate (Corning 4514). The reaction mixtures were collected from 16 replicates and transferred to a nonbinding Eppendorf tube followed by coincubating with 10 μL of 60 μM dithiothreitol (DTT) for 30 min to quench the unreacted CPM. The protein mixture was then purified through Amicon (10K) to exchange the buffer with 50 mM Tris-HCl (pH 7.5).

In-Solution Digestion and Purification. To 50 μL of the protein sample in 50 mM Tris-HCl (pH 7.5), 250 μL of denaturizing/reducing buffer (10 M urea, 1.2 mM TCEP, and 50 mM Tris, pH 7.5) was added and shaken at room temperature (350 rpm, 30 min). Next, 33.3 μL of 50 mM alkylation solution (iodoacetamide prepared in a denaturizing/reducing buffer) was added and shaken (350 rpm) at room temperature for 30 min. Subsequently, 23.5 μL of 1 ng/μL solution of LysC (Wako, 125-05061) was added at 37 °C and shaken (350 rpm) for 1 h, followed by addition of 7.8 μL of 6 ng/μL trypsin (Roche, 03708969001). The mixture was shaken (350 rpm) at 37 °C overnight. The digested samples were stage tip-purified using C18 (octadecyl) tips (3M High Performance Extraction Discs, Empore) using a protocol described earlier.[46] Bovine serum albumin (50 μL, 0.5 μM prepared in 50 mM Tris-HCl, pH 7.5) was used in parallel as a control for the digestion–purification experiments and treated as described above. The peptide solution was injected to NanoLC-MS (ThermoScientific_UltiMate 3000 nanoLC coupled to a QExactive Plus or QExactive HF MS) through a nanocolumn (ThermoScientific PEPMAP C18 2UM 75UMX500MM).

mTEAD4 (Nonacylated) HSCQ Experiments. The $^{13}C/^{15}N$-labeled mTEAD4 was prepared following a protocol established earlier,[45] and the protein was deacylated as described above for hTEAD4. $^{1}H–^{15}N$ HSQC spectra in the presence of DMSO or the test compound (0.5 mM) were collected at 37 °C on a Bruker 600 MHz magnet equipped with a cryoprobe in 20 mM HEPES, pH 7.3 buffer containing 150 mM NaCl and 1 mM DTT. The spectra were processed and overlaid.

CETSA Experiments. *Lysate Preparation.* HCT116 cells were grown in Dulbecco's modified Eagle's medium (Sigma-Aldrich, #P04-03550) containing 10% fetal bovine serum, 1× NEAA (Sigma-Aldrich, # P08-32800) and 1 mM sodium pyruvate (Sigma-Aldrich, #S8636) until they reached 90% confluency. Cells were detached, transferred to two separate tubes, and washed three times with PBS. Then, 0.6 mL of PBS containing 0.04% NP-40 was added to each tube

https://dx.doi.org/10.1021/acs.jmedchem.0c01275
J. Med. Chem. 2020, 63, 11972–11989

and cells were lysed by means of freeze and thaw. Lysates were centrifuged (Beckman Optima MAX-TL) at 100,000*g*, 4 °C for 25 min and protein concentration was determined using the DC Protein Assay Kit I (Bio-Rad, #5000111). Aliquots (1.5 mL) containing 1 mg/mL protein were stored at −80 °C until further usage.

CETSA. Compound **19** (2.75 μL 10 mM stock, 50 μM) or DMSO (2.75 μL) was added to 550 μL of HCT116 lysates (1 mg/mL), samples were mixed and incubated for 10 min at room temperature. Treated and nontreated lysates were divided into ten aliquots, each 50 μL in PCR tubes. The aliquots were individually heated at different temperatures (Eppendorf Mastercycler ep Gradient S). After the heat treatment, the cell lysates were directly completely transferred to polycarbonate tubes and centrifuged (Beckman Optima MAX-TL) at 100,000*g*, 4 °C for 25 min. To 16 μL of each supernatant was added 4 μL of 5× loading buffer and incubated for 5 min at 95 °C, before samples were analyzed by immunoblotting. Proteins were separated by sodium dodecyl sulphate-polyacrylamide gel electrophoresis (SDS-PAGE) and transferred to a polyvinylidene difluoride membrane using wet transfer. The membranes were blocked with Odyssey blocking buffer (TBS; *Li-Cor*) for 1 h and incubated with the primary antibody (Mouse anti-TEAD4 antibody corresponding to amino acids 151−261 of Human TEAD4—ChIP Grade (ab58310)) in Odyssey blocking buffer containing 0.2% Tween 20 at 4 °C overnight. After washing with TBS-T (TBS containing 0.1% Tween 20), the membrane was incubated with the secondary antibody coupled to IRDye 800CW (goat anti-mouse IgG, *Li-COR*) for 1 h, in Odyssey blocking buffer containing 0.2% Tween 20 and 0.1% SDS at room temperature. Membranes were washed with TBS-T and then TBS before images were taken (Bio-Rad ChemiDoc MP Imaging System).

Analysis. Images were analyzed with ImageJ (FUJI). Normalization and all calculations were performed with GraphPad Prism 7 software (Curves: IC_{50} variable slope → turning points correspond to melting temperature in obtained curves).

RNA Purification and RT-qPCR. HEK293 cells were treated with DMSO or the indicated compound for the indicated duration. RNA was extracted using the RNeasy Plus Mini Kit (QIAGEN, Hilden, Germany) following the manufacturer's procedure. DNA was removed on the column by DNase digestion with the RNase-free DNase Set (QIAGEN, Hilden, Germany) according to the manufacturer's instructions. Following the manufacturer's protocol, cDNA templates were synthesized from 700 ng total RNA using the QuantiTect Reverse Transcription Kit (QIAGEN, Hilden, Germany).

The expression levels of the TEAD target gene ANKRD1 was assessed by real-time quantitative PCR. A total of 100 ng of cDNA was amplified using 500 nM gene-specific primers and SsoAdvanced Universal SYBR Green Supermix (Bio-Rad Laboratories, Feldkirchen, Germany) in a total volume of 10 μL for 50 cycles. All measurements were performed in both technical and biological triplicates using a CFX96 Touch Real-Time PCR Detection System (Bio-Rad Laboratories, Feldkirchen, Germany).

The sequences of primers for ANKRD1 were forward 5′-AGACTCCTTCAGCCAACATGATG-3′ and reverse 5′-CTCTCCATCTCTGAAATCCTCAGG-3′. The sequences of primers for GAPDH were forward 5′-GTCTCCTCTGACTTCAACAGCG-3′ and reverse 5′-ACCACCCTGTTGCTGTAGCCAA-3′.

Assay Media Stability. The compounds were incubated in MES (25 mM), pH 6.5 buffer or HEPES (25 mM) and NaCl (150 mM) pH 6.5 buffer for an hour at room temperature before injecting into a reverse-phase HPLC system (ThermoScientific_Ultimate 3000) equipped with a C18 column (2/50 Nucleodur C18 gravity 1.8 μm von Macherey-Nagel).

CHEMISTRY

All the final compounds were characterized with ^{1}H NMR, ^{13}C NMR (500, 700 MHz, Bruker), and HR-MS (ESI^+) (LTQ Orbitrap mass spectrometer). The intermediates were characterized with ^{1}H NMR, ^{13}C NMR (500, 700 MHz, Bruker), and LR-MS (ESI^+) (Agilent 1290 Infinity UPLC/MS coupled to Agilent 6120 Quadripole or ThermoScientific_UltiMate 3000 LCMS coupled to LQC Fleet). Chemical shifts were reported in ppm relative to tetramethylsilane. CD_3OD (3.31 ppm) or DMSO-d_6 (2.50 ppm) was used as the internal standard for ^{1}H NMR spectra. CD_3OD (49.0 ppm) or DMSO-d_6 (39.52 ppm) was used as the internal standard for ^{13}C NMR spectra. All the final compounds have purity ≥95% as determined by reverse-phase UPLC (Agilent 1260 Infinity or ThermoScientific_Dionex Ultimate 3000 LCMS) equipped with a C18 column (Nucleodur C18 Gravity, 5 μm).

Compounds **1**−**3** and **10**−**16** were obtained from commercial sources and used without further purification.

2-((2-Fluorophenyl)(pyridin-2-ylamino)methyl)-3-hydroxy-6-(hydroxymethyl)-4*H*-pyran-4-one (10). Each component (2 mmol) (kojic acid, 2-fluorobenzaldehyde, and 2-amino pyridine) in dimethylformamide (DMF) was stirred at room temperature for 2 days before being concentrated in vacuo. Then, the remaining crude was purified over a silica column using ethyl acetate/methanol (20:1) as an eluent. The collected fractions were concentrated and further washed with methanol yielding compound **10** as a white solid. HRMS (ESI): *m*/*z* calcd for $C_{18}H_{15}FN_2O_4 + H^+$ $[M + H]^+$, 343.1089; found, 343.1089. ^{1}H NMR (500 MHz, DMSO-d_6): δ 9.20 (s, 1H), 7.94 (dd, *J* = 5.2, 1.8 Hz, 1H), 7.51 (td, *J* = 7.8, 1.9 Hz, 1H), 7.44−7.37 (m, 2H), 7.33 (tdd, *J* = 7.4, 5.2, 1.8 Hz, 1H), 7.17 (q, *J* = 9.3, 8.1 Hz, 2H), 6.84 (d, *J* = 8.2 Hz, 1H), 6.68 (d, *J* = 8.4 Hz, 1H), 6.53 (dd, *J* = 7.0, 5.0 Hz, 1H), 6.30 (s, 1H), 5.64 (t, *J* = 6.2 Hz, 1H), 4.31−4.18 (m, 2H).

^{13}C NMR (126 MHz, DMSO): δ 173.8, 167.5, 160.8, 158.8, 157.1, 148.1, 147.4, 141.2, 136.9, 129.5, 129.4, 128.99, 128.96, 126.8, 126.7, 124.5, 124.4, 115.4, 115.3, 112.8, 109.1, 108.9, 59.4, 44.80, 44.77, 40.1, 40.0, 39.94, 39.85, 39.78, 39.7, 39.5, 39.4, 39.2, 39.0.

3-Hydroxy-6-(hydroxymethyl)-2-(phenyl(phenylamino)methyl)-4*H*-pyran-4-one (19). Each component (2 mmol) (kojic acid, benzaldehyde, and aniline) in DMF was stirred at room temperature for 3 days before being concentrated in vacuo. Then, the remaining crude was washed with ethanol yielding compound **19** as a white solid (34% yield). HRMS (ESI): *m*/*z* calcd for $C_{19}H_{17}NO_4 + H^+$ $[M + H]^+$, 324.1230; found, 324.1236. ^{1}H NMR (700 MHz, DMSO-d_6): δ 9.36 (s, 1H), 7.50−7.45 (m, 2H), 7.37 (t, *J* = 7.7 Hz, 2H), 7.32−7.27 (m, 1H), 7.09−7.04 (m, 2H), 6.73−6.68 (m, 2H), 6.60−6.55 (m, 1H), 6.41 (d, *J* = 8.2 Hz, 1H), 6.27 (s, 1H), 5.89 (d, *J* = 8.2 Hz, 1H), 5.61 (t, *J* = 6.3 Hz, 1H), 4.25 (qd, *J* = 15.5, 5.8 Hz, 2H).

^{13}C NMR (176 MHz, DMSO): δ 173.6, 167.5, 148.9, 147.2, 141.5, 139.2, 128.9, 128.6, 127.6, 127.0, 116.9, 112.9, 108.9, 59.4, 52.9.

^{1}H NMR, ^{13}C NMR, purity and assay media stability spectra of compound **19** is shown in Supporting Information (pages S17, S19−S21).

3-Hydroxy-6-(hydroxymethyl)-2-((phenylamino)(*p*-tolyl)methyl)-4*H*-pyran-4-one (20). Each component (1 mmol) (kojic acid, benzaldehyde, and isopropylamine) in 15 mL of EtOH was stirred at room temperature for 7 h before being concentrating in vacuo. The remaining crude was purified using a silica column using ethyl acetate/methanol (25:1) as an eluent. The compound was dissolved in an acetonitrile/H_2O mixture and lyophilized yielding 19 mg of compound **20** (6.5% yield). HRMS (ESI): *m*/*z* calcd for $C_{16}H_{19}NO_4 + H^+$ $[M + H]^+$, 290.1387; found, 290.1391. ^{1}H NMR (700 MHz, DMSO-d_6): δ 7.43−7.40 (m, 2H), 7.33 (dd, *J* = 8.4, 6.9 Hz, 2H), 7.28−7.24 (m, 1H), 6.26 (s, 1H), 5.62 (t,

https://dx.doi.org/10.1021/acs.jmedchem.0c01275
J. Med. Chem. 2020, 63, 11972−11989

J = 6.4 Hz, 1H), 5.16 (s, 1H), 4.31−4.22 (m, 2H), 2.64 (h, J = 6.2 Hz, 1H), 1.01 (dd, J = 10.4, 6.2 Hz, 6H).

^{13}C NMR (176 MHz, DMSO): δ 173.5, 167.1, 150.2, 141.9, 140.5, 128.4, 127.3, 127.1, 108.9, 59.5, 55.8, 45.8, 22.9, 22.3.

2-((Benzylamino)(phenyl)methyl)-3-hydroxy-6-(hydroxymethyl)-4*H*-pyran-4-one (21). Each component (1 mmol) (kojic acid, benzaldehyde, and benzyl amine) in 15 mL of EtOH was stirred at room temperature for 3 days before being concentrated in vacuo. The remaining crude was extracted with ethyl acetate and water. The organic layers were dried over anhydrous $MgSO_4$ and concentrated. The remaining crude was purified using a silica column using ethyl acetate as an eluent. A second silica column purification step was pursued using CH_2Cl_2/MeOH (10:0.75) as an eluent. The purified compound was dissolved in an acetonitrile/H_2O mixture and lyophilized yielding 22 mg of compound **21** as a cream color solid (0.065 mmol, % 65 yield). HRMS (ESI): m/z calcd for $C_{20}H_{19}NO_4$ + H^+ [M + H]$^+$, 338.1387; found, 338.1375. ^{1}H NMR (500 MHz, DMSO-d_6): δ 9.09 (s, 1H), 7.43−7.40 (m, 2H), 7.36−7.25 (m, 7H), 7.24−7.20 (m, 1H), 6.26 (s, 1H), 5.65 (t, J = 6.4 Hz, 1H), 5.06 (s, 1H), 4.27 (qd, J = 15.5, 6.2 Hz, 2H), 3.66 (s, 2H).

^{13}C NMR (126 MHz, DMSO): δ 173.5, 167.2, 149.8, 141.9, 140.3, 140.1, 128.5, 128.14, 128.11, 127.4, 127.1, 126.8, 108.8, 59.5, 57.4, 50.7.

3-Hydroxy-6-(hydroxymethyl)-2-(isoindolin-2-yl(phenyl)methyl)-4*H*-pyran-4-one (22). Each component (1 mmol) (kojic acid, benzaldehyde, and isoindoine) in 15 mL of EtOH was stirred at room temperature overnight before being concentrated in vacuo. The remaining crude was extracted with ethyl acetate and water. The organic layers were dried over anhydrous $MgSO_4$ and concentrated. The remaining crude was purified using a silica column using ethyl acetate as an eluent. Then, the compound was dissolved in an acetonitrile/H_2O mixture and lyophilized yielding 38 mg of compound **22** as an off-white solid (11% yield). HRMS (ESI): m/z calcd for $C_{21}H_{19}NO_4$ + H^+ [M + H]$^+$, 350.1387; found, 350.1369. ^{1}H NMR (700 MHz, DMSO-d_6): δ 9.23 (s, 1H), 7.57−7.54 (m, 2H), 7.38 (t, J = 7.6 Hz, 2H), 7.32 (td, J = 7.1, 1.4 Hz, 1H), 7.22−7.16 (m, 4H), 6.30 (s, 1H), 5.65 (t, J = 6.2 Hz, 1H), 5.19 (s, 1H), 4.35−4.25 (m, 2H), 3.85−3.78 (m, 4H).

^{13}C NMR (176 MHz, DMSO): δ 173.6, 167.7, 148.5, 142.0, 139.4, 139.1, 128.6, 128.1, 127.9, 126.6, 122.3, 108.8, 64.4, 59.5, 57.1.

2-(((3-Fluorophenyl)amino)(phenyl)methyl)-3-hydroxy-6-(hydroxymethyl)-4*H*-pyran-4-one (23). Each component (1 mmol) (kojic acid, benzaldehyde, and 3-fluoroaniline) in 15 mL of EtOH was stirred at room temperature for 5 days before being concentrated in vacuo. The remaining crude was extracted with ethyl acetate and water. The organic layers were dried over anhydrous $MgSO_4$ and concentrated and the remaining crude was purified using a silica column using ethyl acetate as an eluent. Next, the collected fractions were concentrated and washed with CH_2Cl_2. The remaining white powder was dissolved in an acetonitrile/H_2O mixture and lyophilized yielding 46 mg of compound **23** as a cream color solid (0.135 mmol, 13.5% yield). HRMS (ESI): m/z calcd for $C_{19}H_{16}FNO_4$ + H^+ [M + H]$^+$, 342.1136; found, 342.1139. ^{1}H NMR (500 MHz, DMSO-d_6): δ 9.48 (s, 1H), 7.50−7.43 (m, 2H), 7.42−7.35 (m, 2H), 7.34−7.25 (m, 1H), 7.08 (td, J = 8.2, 7.0 Hz, 1H), 6.81 (d, J = 7.9 Hz, 1H), 6.55−6.51 (m, 1H), 6.46 (dt, J = 12.3, 2.3 Hz, 1H), 6.35 (td, J = 8.5, 2.5 Hz, 1H), 6.29 (s, 1H), 5.88 (d, J = 8.0 Hz, 1H), 5.63 (t, J = 6.2 Hz, 1H), 4.30−4.20 (m, 2H).

^{13}C NMR (126 MHz, DMSO): δ 173.6, 167.6, 164.2, 162.3, 149.37, 149.28, 148.3, 141.7, 138.7, 130.45, 130.37, 128.7, 127.8, 127.1, 108.99, 108.98, 108.95, 103.1, 102.9, 99.4, 99.2, 59.4, 52.9.

3-Hydroxy-6-(hydroxymethyl)-2-(phenyl(pyridin-2-ylamino)methyl)-4*H*-pyran-4-one (24). Each component (2 mmol) (kojic acid, benzaldehyde, and 2-aminopyridine) in DMF was stirred at room temperature for 3 days before being concentrated in vacuo. Then, the remaining crude was washed with ethanol yielding compound **24** as a white solid. HRMS (ESI): m/z calcd for $C_{18}H_{16}N_2O_4$ + H^+ [M + H]$^+$, 325.1183; found, 325.1169. ^{1}H NMR (500 MHz, DMSO-d_6): δ 9.25 (s, 1H), 7.95 (dd, J = 5.2, 1.8 Hz, 1H), 7.44−7.31 (m, 6H), 7.28−7.23 (m, 1H), 6.72 (d, J = 8.4 Hz, 1H), 6.67 (d, J = 8.6 Hz, 1H), 6.53 (dd, J = 7.0, 5.1 Hz, 1H), 6.29 (s, 1H), 5.64 (t, J = 6.3 Hz, 1H), 4.28 (qd, J = 15.6, 6.2 Hz, 2H).

^{13}C NMR (126 MHz, DMSO): δ 173.8, 167.4, 157.4, 149.5, 147.4, 141.0, 140.2, 137.0, 128.5, 127.4, 126.8, 112.7, 109.1, 108.9, 59.5, 50.1.

3-Hydroxy-6-(hydroxymethyl)-2-(((4-methylpyridin-2-yl)amino)(phenyl)methyl)-4*H*-pyran-4-one (25). Each component (1 mmol) (kojic acid, benzaldehyde, and 2-amino-4-methylpyridine) in 15 mL of EtOH was stirred at room temperature for 2 days before being concentrated in vacuo. The remaining crude was extracted with ethyl acetate and water. The organic layers were dried over anhydrous $MgSO_4$, concentrated, and dried. The remaining crude was taken in a mixture of ethyl acetate/MeOH (10:0.5) and sonicated for 10 min. The solution was discarded and the wash step was repeated. Next, the step was repeated using EtOH. Then, the compound was taken in an acetonitrile/H_2O mixture and lyophilized yielding 156 mg of compound **25** as a white solid (0.46 mmol, 46% yield). HRMS (ESI): m/z calcd for $C_{19}H_{18}N_2O_4$ + H^+ [M + H]$^+$, 339.1339; found, 339.1325. ^{1}H NMR (500 MHz, DMSO-d_6): δ 9.25 (s, 1H), 7.82 (d, J = 5.2 Hz, 1H), 7.41−7.36 (m, 2H), 7.36−7.30 (m, 2H), 7.29−7.22 (m, 2H), 6.67 (d, J = 8.7 Hz, 1H), 6.54 (d, J = 1.5 Hz, 1H), 6.39 (dd, J = 5.3, 1.4 Hz, 1H), 6.29 (s, 1H), 5.64 (t, J = 6.3 Hz, 1H), 4.28 (qdd, J = 15.6, 6.3, 0.9 Hz, 2H), 2.15 (s, 3H).

^{13}C NMR (126 MHz, DMSO): δ 173.8, 167.4, 157.6, 149.6, 147.23, 147.07, 140.9, 140.3, 128.5, 127.3, 126.8, 114.4, 109.0, 108.9, 59.5, 50.1, 20.6.

3-Hydroxy-6-(hydroxymethyl)-2-(phenyl(pyrimidin-2-ylamino)methyl)-4*H*-pyran-4-one (26). Each component (1 mmol) (kojic acid, benzaldehyde, and 2-aminopyrimidine) in 15 mL of EtOH was stirred at room temperature for 6 days before being concentrated in vacuo. The remaining crude was extracted with ethyl acetate and water. The organic layers together were dried over anhydrous $MgSO_4$, concentrated, and dried. The remaining crude was purified using a silica column using CH_2Cl_2/MeOH (10:0.5) as an eluent. Then, the compound was taken in an acetonitrile/H_2O mixture and lyophilized yielding 8 mg of compound **26** as a white solid (0.025 mmol, 2.5% yield). HRMS (ESI): m/z calcd for $C_{17}H_{15}N_3O_4$ + H^+ [M + H]$^+$, 326.1135; found, 326.1128. ^{1}H NMR (700 MHz, DMSO-d_6): δ 9.29 (s, 1H), 8.33 (d, J = 4.8 Hz, 2H), 8.05 (d, J = 9.1 Hz, 1H), 7.41 (dd, J = 8.0, 1.4 Hz, 2H), 7.34 (t, J = 7.7 Hz, 2H), 7.30−7.22 (m, 1H), 6.69 (d, J = 9.1 Hz, 1H), 6.66 (t, J = 4.8 Hz, 1H), 6.29 (d, J = 0.9 Hz, 1H),

https://dx.doi.org/10.1021/acs.jmedchem.0c01275
J. Med. Chem. 2020, 63, 11972−11989

5.65 (t, J = 6.5 Hz, 1H), 4.29 (dddd, J = 56.1, 15.4, 6.5, 0.9 Hz, 2H).

^{13}C NMR (176 MHz, DMSO): δ 173.8, 167.3, 158.14, 157.99, 148.6, 140.8, 139.8, 128.5, 127.4, 126.6, 111.2, 108.9, 59.5, 50.4.

3-Hydroxy-6-(hydroxymethyl)-2-(phenyl(thiazol-2-ylamino)methyl)-4*H*-pyran-4-one (27). Each component (1 mmol) (kojic acid, benzaldehyde, and thiazol-2-amine) in 15 mL of EtOH was stirred at room temperature for 14 days before being concentrated in vacuo. The remaining crude was extracted with ethyl acetate and water. The organic layers were dried over anhydrous $MgSO_4$, concentrated, and dried. The remaining crude was purified using a silica column using CH_2Cl_2/MeOH (10:1) as an eluent. Then, the compound was dissolved in an acetonitrile/H_2O mixture and lyophilized yielding 34 mg of compound **27** as an off-white solid (10% yield). HRMS (ESI): m/z calcd for $C_{16}H_{14}N_2O_4S$ + H^+ $[M + H]^+$, 331.0747; found, 331.0735. ^{1}H NMR (600 MHz, DMSO-d_6): δ 9.34 (s, 1H), 8.48 (d, J = 8.3 Hz, 1H), 7.42−7.38 (m, 2H), 7.36 (t, J = 7.7 Hz, 2H), 7.31−7.26 (m, 1H), 7.01 (d, J = 3.6 Hz, 1H), 6.67 (d, J = 3.6 Hz, 1H), 6.39 (d, J = 7.9 Hz, 1H), 6.30 (s, 1H), 5.63 (t, J = 6.3 Hz, 1H), 4.34−4.21 (m, 2H).

^{13}C NMR (151 MHz, DMSO): δ 173.7, 167.54, 167.41, 148.3, 141.1, 139.1, 138.4, 128.6, 127.7, 126.8, 109.0, 107.6, 59.4, 53.8.

2-(((1*H*-Benzo[*d*]imidazol-2-yl)amino)(phenyl)-methyl)-3-hydroxy-6-(hydroxymethyl)-4*H*-pyran-4-one (28). Each component (1 mmol) (kojic acid, benzaldehyde, and 1*H*-benzimidazol-2-amine) in 15 mL of EtOH was stirred at room temperature for 20 days before being concentrated in vacuo. The remaining crude was extracted with ethyl acetate and water. The organic layers were dried over anhydrous $MgSO_4$, concentrated, and dried. The remaining crude was taken in a mixture of ethyl acetate/MeOH (10:0.5) and sonicated for 5 min. The solution was discarded, and the wash step was repeated twice. Then, the compound was taken in an acetonitrile/H_2O mixture and lyophilized yielding 22 mg of compound **28** as an off-white solid (0.06 mmol, 6% yield). HRMS (ESI): m/z calcd for $C_{20}H_{17}N_3O_4$ + H^+ $[M + H]^+$, 364.1292; found, 364.1268. ^{1}H NMR (700 MHz, DMSO-d_6): δ 10.69 (bs, 1H), 9.62 (bs, 1H), 7.60 (d, J = 9.1 Hz, 1H), 7.47−7.43 (m, 2H), 7.37 (t, J = 7.6 Hz, 2H), 7.29 (t, J = 7.4 Hz, 1H), 7.17 (d, J = 8.7 Hz, 2H), 6.89 (s, 2H), 6.49 (d, J = 8.5 Hz, 1H), 6.31 (s, 1H), 5.65 (bs, 1H), 4.29 (q, J = 15.4 Hz, 2H).

^{13}C NMR (176 MHz, DMSO): δ 173.9, 167.2, 154.1, 149.0, 141.1, 139.5, 128.6, 127.6, 126.7, 109.2, 59.5, 52.6.

4-(((3-Hydroxy-6-(hydroxymethyl)-4-oxo-4*H*-pyran-2-yl)(phenyl)methyl)amino)benzamide (29). Each component (1 mmol) (kojic acid, benzaldehyde, and 4-aminobenzamide) in 15 mL of EtOH was stirred at room temperature for 3 days before being concentrated in vacuo. The remaining crude was partitioned between ethyl acetate and water. The observed white precipitate from both layers was collected and washed with ethyl acetate and water. The compound was then taken in an acetonitrile/H_2O mixture and lyophilized yielding 95 mg of compound **29** as an off-white solid (26% yield). HRMS (ESI): m/z calcd for $C_{20}H_{18}N_2O_5$ + H^+ $[M + H]^+$, 367.1288; found, 367.1289. ^{1}H NMR (700 MHz, DMSO-d_6): δ 9.46 (s, 1H), 7.65−7.61 (m, 2H), 7.55 (bs, 1H), 7.50−7.45 (m, 2H), 7.38 (t, J = 7.7 Hz, 2H), 7.34−7.30 (m, 1H), 6.94 (d, J = 7.9 Hz, 1H), 6.90 (bs, 1H), 6.71−6.67 (m, 2H), 6.29 (d, J = 0.9 Hz, 1H), 5.96 (d, J = 7.9 Hz, 1H), 5.62 (t, J = 6.3 Hz, 1H), 4.30−4.21 (m, 2H).

^{13}C NMR (176 MHz, DMSO): δ 173.6, 167.8, 167.6, 149.7, 148.3, 141.7, 138.7, 128.96, 128.67, 127.8, 127.1, 122.4, 111.7, 108.9, 59.4, 52.7.

2-(Cyclohexyl(phenylamino)methyl)-3-hydroxy-6-(hydroxymethyl)-4*H*-pyran-4-one (30). Each component (1 mmol) (kojic acid, cyclohexanecarboxaldehyde, and aniline) in 15 mL of EtOH was stirred at room temperature for 5 days before being concentrated in vacuo. The remaining crude was extracted with ethyl acetate and brine. The organic layers were dried over anhydrous $MgSO_4$ and concentrated. The remaining crude was purified using a silica column using ethyl acetate/CH_2Cl_2 (1:1) as an eluent. Then, the compound was dissolved in an acetonitrile/H_2O mixture and lyophilized yielding 80 mg of compound **30** as an off-white solid (0.24 mmol, 24% yield). HRMS (ESI): m/z calcd for $C_{19}H_{23}NO_4$ + H^+ $[M + H]^+$, 330.1700; found, 330.1702. ^{1}H NMR (600 MHz, DMSO-d_6): δ 9.03 (s, 1H), 7.04−6.95 (m, 2H), 6.64−6.56 (m, 2H), 6.52−6.44 (m, 1H), 6.24 (d, J = 0.9 Hz, 1H), 5.88 (d, J = 8.7 Hz, 1H), 5.59 (t, J = 6.3 Hz, 1H), 4.37 (t, J = 9.0 Hz, 1H), 4.25 (qdd, J = 15.4, 6.3, 0.9 Hz, 2H), 2.12−2.05 (m, 1H), 1.84−1.76 (m, 1H), 1.73−1.56 (m, 3H), 1.43 (d, J = 12.8 Hz, 1H), 1.27−1.11 (m, 3H), 1.08−0.95 (m, 2H).

^{13}C NMR (151 MHz, DMSO): δ 173.3, 167.4, 149.6, 148.0, 142.7, 128.9, 116.0, 112.2, 108.7, 59.5, 54.3, 30.0, 29.0, 25.9, 25.4.

3-Hydroxy-6-(hydroxymethyl)-2-(2-methyl-1-(phenylamino)propyl)-4*H*-pyran-4-one (31). Each component (1 mmol) (kojic acid, isobutyraldehyde, and aniline) in 15 mL of EtOH was stirred at room temperature for 5 days before being concentrated in vacuo. The remaining crude was extracted with ethyl acetate and brine. The organic layers were dried over anhydrous $MgSO_4$ and concentrated. The remaining crude was purified using a silica column using ethyl acetate/CH_2Cl_2 (1:1) as an eluent. Then, the compound was dissolved in an acetonitrile/H_2O mixture and lyophilized yielding 75 mg of compound **31** as an off-white solid (0.26 mmol, 26% yield). HRMS (ESI): m/z calcd for $C_{16}H_{19}NO_4$ + H^+ $[M + H]^+$, 290.1387; found, 290.1389. ^{1}H NMR (600 MHz, DMSO-d_6): δ 9.04 (s, 1H), 7.04−6.98 (m, 2H), 6.65−6.59 (m, 2H), 6.50 (tt, J = 7.3, 1.1 Hz, 1H), 6.24 (d, J = 0.9 Hz, 1H), 5.90 (d, J = 8.8 Hz, 1H), 5.59 (t, J = 6.2 Hz, 1H), 4.32−4.18 (m, 3H), 2.09 (dp, J = 9.0, 6.6 Hz, 1H), 1.08 (d, J = 6.6 Hz, 3H), 0.84 (d, J = 6.7 Hz, 3H).

^{13}C NMR (151 MHz, DMSO): δ 173.3, 167.3, 149.8, 147.9, 142.5, 128.9, 116.1, 112.2, 108.7, 59.5, 55.5, 30.8, 20.1, 19.1.

3-Hydroxy-6-(hydroxymethyl)-2-((phenylamino)-methyl)-4*H*-pyran-4-one (32). Each component (1 mmol) (kojic acid, formaldehyde, and aniline) in 15 mL of EtOH was stirred at room temperature for 5 days before being concentrated in vacuo. The remaining crude was purified using a silica column using CH_2Cl_2/MeOH (10:1) as an eluent. Then, the compound was dissolved in an acetonitrile/H_2O mixture and lyophilized yielding 100 mg of compound **32** as a light brown-orange solid (40% yield). HRMS (ESI): m/z calcd for $C_{13}H_{13}NO_4$ + H^+ $[M + H]^+$, 248.0917; found, 248.0918. ^{1}H NMR (500 MHz, DMSO-d_6): δ 9.19 (s, 1H), 7.09−7.01 (m, 2H), 6.67−6.61 (m, 2H), 6.57−6.50 (m, 1H), 6.29 (s, 1H), 6.16 (t, J = 6.1 Hz, 1H), 5.65 (t, J = 6.1 Hz, 1H), 4.26 (dd, J = 6.2, 0.9 Hz, 2H), 4.20 (d, J = 6.0 Hz, 2H).

^{13}C NMR (126 MHz, DMSO): δ 173.6, 167.6, 148.0, 147.8, 142.3, 128.9, 116.3, 112.1, 108.9, 59.5.

https://dx.doi.org/10.1021/acs.jmedchem.0c01275
J. Med. Chem. 2020, 63, 11972−11989

4-((3-Hydroxy-6-(hydroxymethyl)-4-oxo-4*H*-pyran-2-yl)(phenylamino)methyl)benzamide (33). Each component (1 mmol) (kojic acid, 4-formylbenzamide, and aniline) in 25 mL of EtOH was stirred at room temperature for 2 days before being concentrated in vacuo. The remaining crude was extracted with ethyl acetate and water. The organic layers were dried over anhydrous $MgSO_4$, concentrated, and dried. The remaining crude was purified using a silica column using ethyl acetate/MeOH (10:1) as an eluent. Then, the compound was taken in an acetonitrile/H_2O mixture and lyophilized yielding 40 mg of compound **33** as a bright-yellow solid (11% yield). HRMS (ESI): *m/z* calcd for $C_{20}H_{18}N_2O_5$ + H^+ $[M + H]^+$, 367.1288; found, 367.1289. ^{1}H NMR (700 MHz, DMSO-d_6): δ 9.43 (s, 1H), 7.94 (bs, 1H), 7.87−7.83 (m, 2H), 7.56−7.52 (m, 2H), 7.34 (bs, 1H), 7.10−7.05 (m, 2H), 6.73−6.68 (m, 2H), 6.59 (tt, *J* = 7.3, 1.1 Hz, 1H), 6.48 (d, *J* = 8.2 Hz, 1H), 6.28 (d, *J* = 0.9 Hz, 1H), 5.94 (d, *J* = 8.2 Hz, 1H), 5.62 (t, *J* = 6.3 Hz, 1H), 4.30−4.20 (m, 2H).

^{13}C NMR (176 MHz, DMSO): δ 173.6, 167.57, 167.55, 148.4, 147.1, 142.4, 141.6, 133.7, 128.9, 127.8, 126.8, 117.0, 113.0, 108.9, 59.4, 52.8.

3-Hydroxy-6-(hydroxymethyl)-2-((phenylamino)(*p*-tolyl)methyl)-4*H*-pyran-4-one (34). Each component (2 mmol) (kojic acid, 4-methylbenzaldehyde, and aniline) in 15 mL of EtOH was stirred at room temperature for 2 days before being concentrated in vacuo. The remaining crude was purified using a silica column using ethyl acetate as an eluent. The purified compound was further washed with diethyl ether. Then, the compound was dissolved in an acetonitrile/H_2O mixture and lyophilized yielding 0.16 g of compound **34** as a light-brown solid (24% yield). HRMS (ESI): *m/z* calcd for $C_{20}H_{19}NO_4$ + H^+ $[M + H]^+$, 338.1387; found, 338.1390. ^{1}H NMR (700 MHz, DMSO-d_6): δ 9.32 (s, 1H), 7.36 (d, *J* = 8.0 Hz, 2H), 7.17 (d, *J* = 7.9 Hz, 2H), 7.09−7.02 (m, 2H), 6.69 (d, *J* = 8.0 Hz, 2H), 6.57 (t, *J* = 7.3 Hz, 1H), 6.35 (d, *J* = 8.2 Hz, 1H), 6.27 (s, 1H), 5.84 (d, *J* = 8.1 Hz, 1H), 5.61 (t, *J* = 6.3 Hz, 1H), 4.25 (qd, *J* = 15.5, 6.2 Hz, 2H), 2.27 (s, 3H).

^{13}C NMR (176 MHz, DMSO): δ 173.6, 167.5, 149.1, 147.3, 141.4, 136.8, 136.2, 129.13, 128.89, 126.9, 116.8, 112.9, 108.8, 59.4, 52.6, 20.6.

2-((4-Fluorophenyl)(phenylamino)methyl)-3-hydroxy-6-(hydroxymethyl)-4*H*-pyran-4-one (35). Each component (1 mmol) (kojic acid, 4-fluorobenzaldehyde, and aniline) in 15 mL of EtOH was stirred at room temperature for 2 days before being concentrated in vacuo. The remaining crude was extracted with ethyl acetate and water. The organic layers were dried over anhydrous $MgSO_4$, concentrated, and dried. The remaining crude was purified using a silica column using CH_2Cl_2/MeOH (10:1) as an eluent, and the dried solid was further washed with ether. Then, the compound was dissolved in an acetonitrile/H_2O mixture and lyophilized yielding 20 mg of compound **35** as a brown-orange solid (6% yield). HRMS (ESI): *m/z* calcd for $C_{19}H_{16}FNO_4$ + H^+ $[M + H]^+$, 342.1136; found, 342.1139. ^{1}H NMR (500 MHz, DMSO-d_6): δ 9.44 (s, 1H), 7.55−7.48 (m, 2H), 7.20 (t, *J* = 8.9 Hz, 2H), 7.11−7.04 (m, 2H), 6.72−6.65 (m, 2H), 6.58 (td, *J* = 7.3, 1.2 Hz, 1H), 6.45 (d, *J* = 8.2 Hz, 1H), 6.28 (s, 1H), 5.89 (d, *J* = 8.2 Hz, 1H), 5.63 (t, *J* = 6.3 Hz, 1H), 4.32−4.18 (m, 2H).

^{13}C NMR (126 MHz, DMSO): δ 173.6, 167.6, 162.5, 160.6, 148.6, 147.1, 141.5, 135.43, 135.41, 129.14, 129.07, 128.97, 117.0, 115.51, 115.34, 113.0, 108.9, 59.4, 52.3.

2-((4-Bromophenyl)(phenylamino)methyl)-3-hydroxy-6-(hydroxymethyl)-4*H*-pyran-4-one (36). Each component (1 mmol) (kojic acid, 4-bromobenzaldehyde, and aniline) in 15 mL of EtOH was stirred at room temperature for 2 days before being concentrated in vacuo. The remaining crude was extracted with ethyl acetate and water. The organic layers were dried over anhydrous $MgSO_4$ and concentrated. The remaining crude was purified using a silica column using ethyl acetate as an eluent. Then, the compound was dissolved in an acetonitrile/H_2O mixture and lyophilized yielding 21 mg of compound **36** as a light-brown solid (5% yield). HRMS (ESI): *m/z* calcd for $C_{19}H_{16}BrNO_4$ + H^+ $[M + H]^+$, 402.0335; found, 402.0334. ^{1}H NMR (700 MHz, DMSO-d_6): δ 9.44 (s, 1H), 7.59−7.53 (m, 2H), 7.45−7.39 (m, 2H), 7.10−7.04 (m, 2H), 6.70−6.67 (m, 2H), 6.59 (dd, *J* = 7.9, 6.6 Hz, 1H), 6.46 (d, *J* = 8.1 Hz, 1H), 6.28 (s, 1H), 5.87 (d, *J* = 8.1 Hz, 1H), 5.61 (t, *J* = 6.3 Hz, 1H), 4.29−4.18 (m, 2H).

^{13}C NMR (176 MHz, DMSO): δ 173.6, 167.6, 148.3, 147.0, 141.5, 138.7, 131.5, 129.2, 128.9, 120.7, 117.1, 113.0, 108.9, 59.4, 52.4.

3-Hydroxy-6-(hydroxymethyl)-2-((4-isopropylphenyl)(phenylamino)methyl)-4*H*-pyran-4-one (37). Each component (2 mmol) (kojic acid, 4-isopropylbenzaldehyde, and aniline) in 10 mL of EtOH was stirred at room temperature for 2 days before being concentrated in vacuo. The remaining crude was purified using a silica column using ethyl acetate as an eluent. The purified compound was further washed with diethyl ether and dried. Then, the compound was dissolved in an acetonitrile/H_2O mixture and lyophilized yielding 0.3 g of compound **37** as a white-bright yellow solid (41% yield). HRMS (ESI): *m/z* calcd for $C_{22}H_{23}NO_4$ + H^+ $[M + H]^+$, 366.1700; found, 366.1682. ^{1}H NMR (700 MHz, DMSO-d_6): δ 9.32 (s, 1H), 7.41−7.38 (m, 2H), 7.25−7.23 (m, 2H), 7.08−7.04 (m, 2H), 6.71−6.68 (m, 2H), 6.57 (tt, *J* = 7.3, 1.2 Hz, 1H), 6.35 (d, *J* = 8.2 Hz, 1H), 6.27 (s, 1H), 5.84 (d, *J* = 8.1 Hz, 1H), 5.62 (t, *J* = 6.3 Hz, 1H), 4.30−4.22 (m, 2H), 2.86 (hept, *J* = 6.9 Hz, 1H), 1.18 (d, *J* = 7.0 Hz, 6H).

^{13}C NMR (176 MHz, DMSO): δ 173.5, 167.4, 149.0, 147.8, 147.3, 141.5, 136.6, 128.9, 127.1, 126.5, 116.8, 112.8, 108.9, 59.4, 52.7, 33.1, 23.85, 23.80.

3-Hydroxy-6-(hydroxymethyl)-2-(naphthalen-2-yl(phenylamino)methyl)-4*H*-pyran-4-one (38). Each component (1 mmol) (kojic acid, 2-naphthaldehyde, and aniline) in 15 mL of EtOH was stirred at room temperature for 2 days before being concentrated in vacuo. The remaining crude was extracted with ethyl acetate and water. The organic layers were dried over anhydrous $MgSO_4$ and concentrated. The remaining crude was purified using a silica column using ethyl acetate as an eluent. Then, the compound was dissolved in an acetonitrile/H_2O mixture and lyophilized yielding 10 mg of compound **38** as a cream color solid (3% yield). HRMS (ESI): *m/z* calcd for $C_{23}H_{19}NO_4$ + H^+ $[M + H]^+$, 374.1387; found, 374.1388. ^{1}H NMR (700 MHz, DMSO-d_6): δ 9.43 (s, 1H), 8.00 (d, *J* = 1.8 Hz, 1H), 7.94−7.88 (m, 3H), 7.62 (dd, *J* = 8.5, 1.8 Hz, 1H), 7.51 (qd, *J* = 7.2, 3.4 Hz, 2H), 7.08 (dd, *J* = 8.4, 7.1 Hz, 2H), 6.75 (d, *J* = 8.0 Hz, 2H), 6.58 (t, *J* = 7.3 Hz, 1H), 6.55 (d, *J* = 8.0 Hz, 1H), 6.28 (s, 1H), 6.06 (d, *J* = 8.0 Hz, 1H), 5.61 (t, *J* = 6.3 Hz, 1H), 4.26 (qd, *J* = 15.6, 6.2 Hz, 2H).

^{13}C NMR (176 MHz, DMSO): δ 173.6, 167.6, 148.8, 147.3, 141.6, 136.8, 132.8, 132.4, 128.9, 128.3, 127.84, 127.50, 126.34, 126.11, 125.5, 125.2, 116.9, 113.0, 108.9, 59.4, 53.1.

2-((2-Fluorophenyl)(phenylamino)methyl)-3-hydroxy-6-(hydroxymethyl)-4*H*-pyran-4-one (39). Each

https://dx.doi.org/10.1021/acs.jmedchem.0c01275
J. Med. Chem. 2020, 63, 11972−11989

component (1 mmol) (kojic acid, 2-fluorobenzaldehyde, and aniline) in 15 mL of EtOH was stirred at room temperature for 5 days before being concentrated in vacuo. The remaining crude was extracted with ethyl acetate and brine. The organic layers were dried over anhydrous $MgSO_4$ and concentrated. The remaining crude was purified using a silica column using ethyl acetate as an eluent. Then, the compound was dissolved in an acetonitrile/H_2O mixture and lyophilized yielding 135 mg of compound **39** as an off-white solid (40% yield). HRMS (ESI): m/z calcd for $C_{19}H_{16}FNO_4 + H^+$ $[M + H]^+$, 342.1136; found, 342.1139. ^{1}H NMR (700 MHz, DMSO-d_6): δ 9.29 (s, 1H), 7.55 (td, J = 7.8, 1.8 Hz, 1H), 7.29 (tdd, J = 7.5, 5.3, 1.8 Hz, 1H), 7.17−7.12 (m, 2H), 7.03−6.98 (m, 2H), 6.59 (d, J = 8.0 Hz, 2H), 6.52 (t, J = 7.3 Hz, 1H), 6.39 (d, J = 8.0 Hz, 1H), 6.22 (s, 1H), 6.07 (d, J = 8.0 Hz, 1H), 5.56 (t, J = 6.2 Hz, 1H), 4.24−4.15 (m, 2H).

^{13}C NMR (176 MHz, DMSO): δ 173.7, 167.6, 160.4, 159.0, 147.4, 146.9, 141.5, 129.78, 129.73, 129.13, 129.11, 129.0, 125.85, 125.77, 124.63, 124.61, 117.1, 115.45, 115.33, 112.7, 108.9, 59.4, 46.56, 46.54.

3-Hydroxy-6-(hydroxymethyl)-2-((phenylamino)-(pyridin-2-yl)methyl)-4*H*-pyran-4-one (40). Each component (1 mmol) (kojic acid, 2-pyridinecarboxaldehyde, and aniline) in 15 mL of EtOH was stirred at room temperature for 2 days before being concentrated in vacuo. The remaining crude was extracted with ethyl acetate and water. The organic layers were dried over anhydrous $MgSO_4$ and concentrated. The remaining crude was purified using a silica column using ethyl acetate as an eluent. Then, the compound was dissolved in an acetonitrile/H_2O mixture and lyophilized yielding 43 mg of compound **40** as a bright-yellow solid (13% yield). HRMS (ESI): m/z calcd for $C_{18}H_{16}N_2O_4 + H^+$ $[M + H]^+$, 325.1183; found, 325.1188. ^{1}H NMR (700 MHz, DMSO-d_6): δ 9.37 (s, 1H), 8.56−8.53 (m, 1H), 7.82 (td, J = 7.7, 1.8 Hz, 1H), 7.56 (d, J = 7.9 Hz, 1H), 7.36−7.31 (m, 1H), 7.11−7.06 (m, 2H), 6.72 (d, J = 8.0 Hz, 2H), 6.59 (t, J = 7.3 Hz, 1H), 6.49 (d, J = 8.0 Hz, 1H), 6.26 (s, 1H), 5.99 (d, J = 8.0 Hz, 1H), 5.59 (t, J = 6.3 Hz, 1H), 4.23−4.13 (m, 2H).

^{13}C NMR (176 MHz, DMSO): δ 173.6, 167.5, 157.8, 148.9, 148.4, 147.0, 142.3, 137.2, 129.0, 123.0, 121.9, 117.0, 112.9, 108.8, 59.4, 54.7.

4-(((3-Hydroxy-6-(hydroxymethyl)-4-oxo-4*H*-pyran-2-yl)(pyridin-2-yl)methyl)amino)benzamide (41). Each component (1 mmol) (kojic acid, 2-pyridinecarboxaldehyde, and 4-aminobenzamide) in 15 mL of EtOH was stirred at room temperature for 3 days before being concentrated in vacuo. The remaining crude was extracted with ethyl acetate and water. The organic layers were dried over anhydrous MgSO4, concentrated, and dried. The crude was then taken in a mixture of ethyl acetate/MeOH (10:1) and sonicated for 5 min. The solution was discarded and the wash step was repeated with ethyl acetate. Then, the compound was taken in an acetonitrile/H_2O mixture and lyophilized yielding 235 mg of compound **41** as a cream color solid (64% yield). HRMS (ESI): m/z calcd for $C_{19}H_{17}N_3O_5 + H^+$ $[M + H]^+$, 368.1241; found, 368.1242. ^{1}H NMR (700 MHz, DMSO-d_6): δ 9.46 (s, 1H), 8.56 (ddd, J = 4.8, 1.8, 0.9 Hz, 1H), 7.83 (td, J = 7.7, 1.8 Hz, 1H), 7.66−7.63 (m, 2H), 7.57 (bs, 1H), 7.54 (dd, J = 8.0, 1.2 Hz, 1H), 7.35 (ddd, J = 7.5, 4.8, 1.1 Hz, 1H), 7.01 (d, J = 7.8 Hz, 1H), 6.91 (bs, 1H), 6.73−6.69 (m, 2H), 6.28 (d, J = 1.0 Hz, 1H), 6.06 (d, J = 7.7 Hz, 1H), 5.59 (t, J = 6.2 Hz, 1H), 4.25−4.11 (m, 2H).

^{13}C NMR (176 MHz, DMSO): δ 173.6, 167.78, 167.64, 157.2, 149.5, 149.0, 147.9, 142.4, 137.3, 129.0, 123.1, 122.5, 122.0, 111.7, 108.9, 59.4, 54.5.

2-((4-Bromophenyl)(pyridin-2-ylamino)methyl)-3-hydroxy-6-(hydroxymethyl)-4*H*-pyran-4-one (42). Each component (2 mmol) (kojic acid, 4-bromobenzaldehyde, and 2-aminopyridine) in DMF was stirred at room temperature for 3 days before being concentrated in vacuo. Then, the remaining crude was washed with ethanol yielding compound **42** as a white solid. HRMS (ESI): m/z calcd for $C_{18}H_{15}BrN_2O_4 + H^+$ $[M + H]^+$, 403.0288; found, 403.0259. ^{1}H NMR (700 MHz, DMSO-d_6): δ 9.31 (s, 1H), 7.95 (ddd, J = 5.1, 1.9, 0.9 Hz, 1H), 7.55−7.52 (m, 2H), 7.43 (ddd, J = 8.8, 7.1, 1.9 Hz, 1H), 7.39 (d, J = 8.5 Hz, 1H), 7.35−7.32 (m, 2H), 6.71 (dt, J = 8.4, 1.0 Hz, 1H), 6.64 (d, J = 8.5 Hz, 1H), 6.55 (ddd, J = 7.0, 5.1, 1.0 Hz, 1H), 6.30−6.29 (m, 1H), 5.62 (t, J = 6.3 Hz, 1H), 4.32−4.22 (m, 2H).

^{13}C NMR (176 MHz, DMSO): δ 173.8, 167.5, 157.2, 148.8, 147.3, 141.0, 139.6, 137.0, 131.4, 128.9, 120.4, 112.9, 109.1, 108.9, 59.4, 49.7.

3-Hydroxy-6-(hydroxymethyl)-2-(pyridin-2-yl-(pyridin-2-ylamino)methyl)-4*H*-pyran-4-one (43). Each component (1 mmol) (kojic acid, 2-pyridinecarboxaldehyde, and 2-aminopyridine) in 15 mL of EtOH was stirred at room temperature for 1 day before being concentrated in vacuo. The remaining crude was extracted with ethyl acetate and water. The organic layers were dried over anhydrous $MgSO_4$, concentrated, and dried. The remaining crude was purified using a silica column using ethyl acetate/MeOH (1:2) as an eluent. Then, the compound was taken in an acetonitrile/H_2O mixture and lyophilized yielding 75 mg of compound **43** as an off-white solid (23% yield). HRMS (ESI): m/z calcd for $C_{17}H_{15}N_3O_4 + H^+$ $[M + H]^+$, 326.1135; found, 326.1122. ^{1}H NMR (700 MHz, DMSO-d_6): δ 9.21 (s, 1H), 8.51 (ddd, J = 4.9, 1.8, 0.9 Hz, 1H), 7.95 (ddd, J = 5.1, 1.9, 0.9 Hz, 1H), 7.78 (td, J = 7.7, 1.8 Hz, 1H), 7.46 (dt, J = 8.0, 1.0 Hz, 1H), 7.43 (ddd, J = 8.7, 7.0, 1.9 Hz, 1H), 7.37 (d, J = 8.3 Hz, 1H), 7.29 (ddd, J = 7.5, 4.8, 1.1 Hz, 1H), 6.76 (dt, J = 8.4, 1.0 Hz, 1H), 6.69 (d, J = 8.3 Hz, 1H), 6.55 (ddd, J = 7.0, 5.0, 1.0 Hz, 1H), 6.28 (d, J = 0.9 Hz, 1H), 5.60 (t, J = 6.3 Hz, 1H), 4.28−4.14 (m, 2H).

^{13}C NMR (176 MHz, DMSO): δ 173.8, 167.4, 158.6, 157.3, 149.11, 148.87, 147.3, 141.8, 136.99, 136.97, 122.6, 121.6, 112.8, 109.1, 108.9, 59.4, 52.3.

3-Hydroxy-6-(hydroxymethyl)-2-((pyridin-2-ylamino)(pyridin-3-yl)methyl)-4*H*-pyran-4-one (44). Each component (1 mmol) (kojic acid, 3-pyridinecarboxaldehyde, and 2-aminopyridine) in 15 mL of EtOH was stirred at room temperature for 2 days before being concentrated in vacuo. The remaining crude was extracted with ethyl acetate and water. The organic layers were dried over anhydrous $MgSO_4$, concentrated, and dried. The remaining crude was purified using a silica column using ethyl CH_2Cl_2/MeOH (20:1) as an eluent. The crude was then washed with ethyl acetate and sonicated. The wash step was repeated two more times. Then, the compound was taken in an acetonitrile/H_2O mixture and lyophilized yielding 110 mg of compound **44** as a cream color solid (34% yield). HRMS (ESI): m/z calcd for $C_{17}H_{15}N_3O_4 + H^+$ $[M + H]^+$, 326.1135; found, 326.1122. ^{1}H NMR (700 MHz, DMSO-d_6): δ 9.21 (s, 1H), 8.51 (ddd, J = 4.9, 1.9, 0.9 Hz, 1H), 7.95 (ddd, J = 5.1, 1.9, 0.8 Hz, 1H), 7.78 (td, J = 7.7, 1.8 Hz, 1H), 7.46 (dd, J = 8.1, 1.3 Hz, 1H), 7.43 (ddd, J = 8.6, 7.0, 1.9 Hz, 1H), 7.37 (d, J = 8.4 Hz, 1H), 7.29

https://dx.doi.org/10.1021/acs.jmedchem.0c01275
J. Med. Chem. 2020, 63, 11972−11989

(ddd, J = 7.5, 4.8, 1.2 Hz, 1H), 6.76 (dt, J = 8.4, 1.0 Hz, 1H), 6.69 (d, J = 8.3 Hz, 1H), 6.55 (ddd, J = 7.1, 5.0, 1.0 Hz, 1H), 6.28 (d, J = 1.0 Hz, 1H), 5.60 (t, J = 6.3 Hz, 1H), 4.26−4.14 (m, 2H).

^{13}C NMR (176 MHz, DMSO): δ 173.8, 167.4, 158.6, 157.3, 149.1, 148.9, 147.3, 141.8, 137.00, 136.97, 122.6, 121.6, 112.8, 109.10, 108.88, 59.4, 52.3.

6-(Hydroxymethyl)-3-methoxy-2-(phenyl-(phenylamino)methyl)-4*H*-pyran-4-one (45). To a stirring solution of 33 mg (0.1 mmol) of compound **19** and 13.8 mg of K_2CO_3 (1 equiv) in 1 mL DMF, 14.1 mg (1 equiv) of iodomethane in 1 mL of DMF was added and stirred for 1 day in ambient temperature. The reaction mixture was then filtered and concentrated. The remaining crude was purified using a silica column using CH_2Cl_2/MeOH (10:0.5) as an eluent yielding 29 mg of white powder (86% yield). HRMS (ESI): m/z calcd for $C_{20}H_{19}NO_4$ + H^+ $[M + H]^+$, 338.1387; found, 338.1379. ^{1}H NMR (500 MHz, DMSO-d_6): δ 7.54−7.49 (m, 2H), 7.42−7.37 (m, 2H), 7.34−7.29 (m, 1H), 7.09 (dd, J = 8.6, 7.2 Hz, 2H), 6.75−6.71 (m, 2H), 6.60 (tt, J = 7.3, 1.1 Hz, 1H), 6.46 (d, J = 8.5 Hz, 1H), 6.27 (d, J = 1.0 Hz, 1H), 5.94 (d, J = 8.5 Hz, 1H), 5.67 (t, J = 6.3 Hz, 1H), 4.32−4.20 (m, 2H), 3.79 (s, 3H).

^{13}C NMR (126 MHz, DMSO): δ 174.5, 167.8, 158.0, 147.1, 143.3, 138.8, 129.0, 128.7, 127.9, 127.2, 117.2, 113.2, 111.7, 59.9, 59.2, 53.4.

^{1}H NMR, ^{13}C- NMR, purity and assay media stability spectra of compound **45** is shown in Supporting Information (pages S18−S21).

2-((2-Fluorophenyl)(pyridin-2-ylamino)methyl)-6-(hydroxymethyl)-3-methoxy-4*H*-pyran-4-one (46). To a stirring solution of 25 mg (0.067 mmol) of compound **10** and 9.3 mg of K_2CO_3 (0.063 mmol) in 1 mL DMF, 4.5 mg (0.5 equiv) of iodomethane in 1 mL DMF was added and stirred for 30 min. Then, another portion of 4.5 mg (0.5 equiv) of iodomethane in 0.5 mL of DMF was added and stirred for 30 min. The reaction mixture was then concentrated. The remaining crude was purified using a silica column using ethyl acetate as an eluent yielding 10 mg (0.028 mmol) of compound **46** as a white powder (42% yield). HRMS (ESI): m/z calcd for $C19H17FN2O4$ + H^+ $[M + H]^+$, 357.1245; found, 357.1222. ^{1}H NMR (500 MHz, DMSO-d_6): δ 7.97 (dd, J = 5.2, 1.8 Hz, 1H), 7.56 (td, J = 7.8, 1.9 Hz, 1H), 7.47 (d, J = 8.3 Hz, 1H), 7.43 (ddd, J = 8.7, 7.0, 2.0 Hz, 1H), 7.39−7.33 (m, 1H), 7.24−7.18 (m, 2H), 6.90 (d, J = 8.3 Hz, 1H), 6.71 (d, J = 8.3 Hz, 1H), 6.58−6.53 (m, 1H), 6.29 (s, 1H), 5.69 (t, J = 6.2 Hz, 1H), 4.30−4.20 (m, 2H), 3.69 (s, 3H).

^{13}C NMR (126 MHz, DMSO): δ 174.7, 167.8, 160.7, 158.7, 157.7, 157.0, 147.4, 143.0, 137.0, 129.86, 129.80, 129.08, 129.06, 126.27, 126.16, 124.67, 124.64, 115.55, 115.38, 113.0, 111.8, 109.3, 59.34, 59.23, 44.82, 44.78.

***tert*-Butyl(3-(2-(2-(3-aminopropoxy)ethoxy)ethoxy)-propyl)carbamate (S2).** Synthesis of **S2** was achieved using the procedure as described earlier.[47] To a solution of 1.01 g (4.6 mmol) of 1,13-diamino-4,7,10-trioxatridecane (**S1**) in 20 mL of dry CH_2Cl_2, 0.5 g (2.3 mmol) of di-*tert*-butyl dicarbonate in 10 mL of dry CH_2Cl_2 was added dropwise over 1 h and stirred at room temperature for overnight. Then, the reaction mixture was washed with H_2O three times, dried over anhydrous $MgSO_4$, and concentrated in vacuo. The remaining colorless oil was used without further purification.

***tert*-Butyl(15-oxo-4,7,10-trioxa-14-azatriacontyl)-carbamate (S3).** Intermediate **S2** (30 mg, 0.1 mmol) was added to a solution of palmitic acid (38.5 mg, 0.15 mmol), EDCI (29 mg, 0.15 mmol), HOAt (20 mg, 0.15 mmol), and DIPEA (26 μL, 0.15 mmol) in 10 mL CH_2Cl_2, and the reaction mixture was stirred at room temperature for 4 h. Then, the reaction was quenched with H_2O and extracted to CH_2Cl_2. The organic phase was dried over anhydrous $MgSO_4$ and concentrated in vacuo. The remaining crude was purified over a silica column using *n*-Hex−EtAc (1:1, then 1:4, then Et Ac only) as an eluent. **S3** was obtained as a white solid (60 mg, 0.11 mmol, 98% yield). LRMS (ESI): m/z calcd for $C_{31}H_{62}N_2O_6$ + H^+ $[M + H]^+$, 559.47; found, 559.06. ^{1}H NMR (500 MHz, methanol-d_4): δ 3.64 (dp, J = 5.1, 2.4 Hz, 4H), 3.59 (dq, J = 7.0, 3.7, 3.0 Hz, 4H), 3.51 (td, J = 6.1, 4.2 Hz, 4H), 3.25 (t, J = 6.8 Hz, 2H), 3.12 (t, J = 6.8 Hz, 2H), 2.17 (t, J = 7.5 Hz, 2H), 1.74 (dp, J = 17.2, 6.5 Hz, 4H), 1.60 (q, J = 7.2 Hz, 2H), 1.43 (s, 9H), 1.36−1.25 (m, 24H), 0.90 (t, J = 6.9 Hz, 3H).

^{13}C NMR (126 MHz, MeOD): δ 176.3, 158.5, 79.8, 71.6, 71.26, 71.25, 69.89, 69.86, 38.7, 37.8, 37.2, 33.1, 30.91, 30.83, 30.81, 30.79, 30.75, 30.67, 30.51, 30.47, 30.43, 30.32, 28.8, 27.1, 23.8, 14.5.

2-(6-Hydroxy-3-oxoi-3H-xanthen-9-yl)-5-(3-(15-oxo-4,7,10-trioxa-14-azatriacontyl)thioureido)benzoic Acid (S4). A total of 2 mL of 4 M HCl solution in 1,4-dioxane was added to a solution of **S3** (10 mg, 0.017 mmol) in 10 mL of MeOH and was stirred at room temperature overnight. Then, the reaction mixture was concentrated, the remaining crude (7.4 mg, 0.015 mmol) was added into 2 mL of DMF, and DIPEA (7.8 μL, 0.045 mmol, 3 equiv) was added followed by FITC addition (8.2 mg, 0.021 mmol, 1.4 equiv) in 1 mL of DMF. The reaction mixture was stirred at room temperature overnight. Then, the solvent was evaporated and the remaining crude was purified over reverse-phase HPLC-MS (Agilent 1260 Infinity coupled to Agilent 6120 Quadripole), with a C18 reverse-phase column (VP125/21 Nucleodur C18 Gravity, 5 μm). **S4** was taken in a mixture of acetonitrile/H_2O and lyophilized yielding 5 mg of orange powder (43% yield). HRMS (ESI): m/z calcd for $C_{47}H_{65}N_3O_9S$ + H^+ $[M + H]^+$, 848.4514; found, 848.4467. ^{1}H NMR (500 MHz, methanol-d_4): δ 8.14 (d, J = 2.0 Hz, 1H), 7.79 (d, J = 8.3 Hz, 1H), 7.17 (d, J = 8.2 Hz, 1H), 6.82−6.66 (m, 4H), 6.65−6.48 (m, 2H), 3.74 (s, 2H), 3.63 (qq, J = 5.0, 3.3, 2.5 Hz, 8H), 3.56 (dd, J = 5.8, 3.3 Hz, 2H), 3.49 (t, J = 6.2 Hz, 2H), 3.23 (t, J = 6.9 Hz, 2H), 2.15 (t, J = 7.5 Hz, 2H), 1.93 (p, J = 6.2 Hz, 2H), 1.73 (p, J = 6.5 Hz, 2H), 1.57 (t, J = 7.3 Hz, 3H), 1.28 (d, J = 9.6 Hz, 23H), 0.89 (t, J = 6.9 Hz, 3H). ^{13}C NMR (176 MHz, MeOD): δ 182.6, 176.3, 171.2, 154.2, 142.4, 130.3, 113.6, 111.5, 103.5, 71.52, 71.44, 71.23, 71.14, 70.4, 69.9, 37.8, 37.2, 33.1, 30.80, 30.79, 30.76, 30.72, 30.63, 30.48, 30.45, 30.44, 30.30, 29.9, 27.1, 23.7, 14.4.

Synthesis of FITC-YAP$^{50-100}$. The YAP peptide (Fmoc-A G H Q I V H V R G D S E T D L E A L F N A V M N P K-TANVPQTVPMRLRKLPDSFFKPPE) was synthesized on a Syro I peptide synthesizer (Multisyntech) following standard Fmoc-protocols for solid-phase peptide synthesis using Rink amide ChemMatrix resin (Aldrich, 0.28 mmol/g, 0.05 mmol). The N-terminal Fmoc group in the resulting peptide on the resin was deprotected using 25% piperidine and reacted with Fmoc-O_2Oc-OH (0.2 mmol, 4 equiv), HATU (0.2 mmol, 4 equiv), and DIPEA (0.4 mmol, 8 equiv) in DMF for 2 h. The N-terminal Fmoc group was then deprotected followed by the reaction with 5-isothiocyanatefluorescein (0.250 mmol, 5 equiv) and DIPEA (0.5 mmol, 10 equiv) in DMF at room

https://dx.doi.org/10.1021/acs.jmedchem.0c01275
J. Med. Chem. 2020, 63, 11972−11989

temperature for 3 h in the dark. The resin was washed and the coupling procedure was repeated for an additional time and this time shaken in the dark at rt for 16 h. The peptidyl resin (0.05 mmol, 1 equiv) was cleaved with 1 mL of cleavage solution (triisopropylsilane 2.5%, water 2.5% in trifluoroacetyl) for 3 h at room temperature. The peptide was precipitated in 40 mL of cold diethyl ether/petroleum ether (1:1) upon 10 min of centrifugation. The pellet was washed twice with 40 mL of diethyl ether. The crude was dried over vacuum, dissolved in water, and lyophilized. Then, the crude was dissolved in 1 mL of DMSO and the peptide was purified by reverse-phase HPLC. HRMS (ESI): m/z calcd for $C_{280}H_{425}N_{75}O_{81}S_3$ + $[M + 5H]^{5+}$, 1247.0194; found, 1247.0158 calcd for +$[M + 6H]^{6+}$, 1039.3507; found, 1039.3481; calcd for +$[M + 7H]^{7+}$, 891.0159; found, 891.0145.

■ ASSOCIATED CONTENT

Supporting Information

The Supporting Information is available free of charge at https://pubs.acs.org/doi/10.1021/acs.jmedchem.0c01275.

Full-protein ESI−MS analysis of recombinant hTEAD4 (acylated), hTEAD4 (nonacylated), and hTEAD4 (nonacylated) reaction with CPM; tandem-MS analysis of the hTEAD4 (nonacylated) reaction with CPM; competitive inhibition of the thiol conjugation signal with TED-347; saturation binding curve of FITC-palmitate to hTEAD4 (nonacylated) and competitive inhibition curve of niflumic acid (**2**) in the FP assay; time- and concentration-dependent inhibition of hTEAD4; specificity of **19** for TEAD homologues; $^{1}H-^{15}N$ HSQC spectrum of mTEAD4 (nonacylated) treated with **19** or **45**; saturation binding curves of FITC-labeled YAP^{50-100} with TEAD4 proteins; sequences of the TEAD proteins used in the study; scheme for the synthesis of FITC-palmitate; and ^{1}H NMR, ^{13}C NMR, and UPLC spectra of compounds **19** and **45** (PDF)

Molecular formula strings with biological data (CSV)

■ AUTHOR INFORMATION

Corresponding Author

Herbert Waldmann − *Department of Chemical Biology, Max Planck Institute of Molecular Physiology, 44227 Dortmund, Germany; Faculty of Chemistry and Chemical Biology, Technical University Dortmund, 44227 Dortmund, Germany;* orcid.org/0000-0002-9606-7247; Phone: (+49)-231-133-2400; Email: herbert.waldmann@mpi-dortmund.mpg.de; Fax: (+49)-231-133-2499

Authors

Hacer Karatas − *Department of Chemical Biology, Max Planck Institute of Molecular Physiology, 44227 Dortmund, Germany;* orcid.org/0000-0002-7577-0320

Mohammad Akbarzadeh − *Department of Chemical Biology, Max Planck Institute of Molecular Physiology, 44227 Dortmund, Germany*

Hélène Adihou − *Department of Chemical Biology, AstraZeneca−Max Planck Institute Satellite Unit, 44227 Dortmund, Germany; Medicinal Chemistry, Research and Early Development Cardiovascular, Renal and Metabolism, BioPharmaceuticals R&D, AstraZeneca, SE-431 83 Gothenburg, Sweden*

Gernot Hahne − *Department of Chemical Biology, Max Planck Institute of Molecular Physiology, 44227 Dortmund, Germany*

Ajaybabu V. Pobbati − *Institute of Molecular and Cell Biology, A*STAR, 138673 Singapore, Singapore;* orcid.org/0000-0001-5744-265X

Elizabeth Yihui Ng − *Experimental Drug Development Centre (EDDC), Agency for Science, Technology and Research (A*STAR), 138670, Singapore*

Stéphanie M. Guéret − *Department of Chemical Biology, AstraZeneca−Max Planck Institute Satellite Unit, 44227 Dortmund, Germany; Medicinal Chemistry, Research and Early Development Cardiovascular, Renal and Metabolism, BioPharmaceuticals R&D, AstraZeneca, SE-431 83 Gothenburg, Sweden;* orcid.org/0000-0001-7220-9506

Sonja Sievers − *Department of Chemical Biology, Max Planck Institute of Molecular Physiology, 44227 Dortmund, Germany*

Axel Pahl − *Department of Chemical Biology, Max Planck Institute of Molecular Physiology, 44227 Dortmund, Germany*

Malte Metz − *Department of Chemical Biology, Max Planck Institute of Molecular Physiology, 44227 Dortmund, Germany*

Sarah Zinken − *Department of Chemical Biology, Max Planck Institute of Molecular Physiology, 44227 Dortmund, Germany; Faculty of Chemistry and Chemical Biology, Technical University Dortmund, 44227 Dortmund, Germany*

Lara Dötsch − *Department of Chemical Biology, Max Planck Institute of Molecular Physiology, 44227 Dortmund, Germany; Faculty of Chemistry and Chemical Biology, Technical University Dortmund, 44227 Dortmund, Germany*

Christine Nowak − *Department of Chemical Biology, Max Planck Institute of Molecular Physiology, 44227 Dortmund, Germany*

Sasikala Thavam − *Department of Chemical Biology, Max Planck Institute of Molecular Physiology, 44227 Dortmund, Germany*

Alexandra Friese − *Department of Chemical Biology, Max Planck Institute of Molecular Physiology, 44227 Dortmund, Germany*

CongBao Kang − *Experimental Drug Development Centre (EDDC), Agency for Science, Technology and Research (A*STAR), 138670, Singapore;* orcid.org/0000-0002-9886-9374

Wanjin Hong − *Institute of Molecular and Cell Biology, A*STAR, 138673 Singapore, Singapore*

Complete contact information is available at: https://pubs.acs.org/10.1021/acs.jmedchem.0c01275

Notes

The authors declare no competing financial interest.

■ ACKNOWLEDGMENTS

We thank Max Planck Institute of Molecular Physiology Dortmund Protein Facility (DPF) for the expression and purification of hTEAD4 and mTEAD4_Cys360Ala and purification of mTEAD4_Cys360Ser proteins.

■ ABBREVIATIONS

Ala, alanine; brs, broad signal; CPM, *N*-(4-(7-diethylamino-4-methylcoumarin-3-yl)phenyl)maleimide; Cys, cysteine; ESI−MS, electron spray ionization−mass spectrometry; FITC, fluorescein isothiocyanate; FP, fluorescence polarization; mTEAD4, mouse TEAD4; Phe, phenylalanine; Ser, serine;

TEAD, transcriptional-enhanced associate domain; T_m, melting temperature; YAP, yes-associated protein

REFERENCES

(1) Holden, J. K.; Cunningham, C. N. Targeting the hippo pathway and cancer through the TEAD family of transcription factors. *Cancers* **2018**, *10*, 81.

(2) Huh, H.; Kim, D.; Jeong, H.-S.; Park, H. Regulation of TEAD transcription factors in cancer biology. *Cells* **2019**, *8*, 600.

(3) Lin, K. C.; Park, H. W.; Guan, K.-L. Regulation of the hippo pathway transcription factor TEAD. *Trends Biochem. Sci.* **2017**, *42*, 862−872.

(4) Zhou, Y.; Huang, T.; Cheng, A. S.; Yu, J.; Kang, W.; To, K. F. The TEAD family and its oncogenic role in promoting tumorigenesis. *Int. J. Mol. Sci.* **2016**, *17*, 138.

(5) Knight, J. F.; Shepherd, C. J.; Rizzo, S.; Brewer, D.; Jhavar, S.; Dodson, A. R.; Cooper, C. S.; Eeles, R.; Falconer, A.; Kovacs, G.; Garrett, M. D.; Norman, A. R.; Shipley, J.; Hudson, D. L. TEAD1 and c-Cbl are novel prostate basal cell markers that correlate with poor clinical outcome in prostate cancer. *Br. J. Cancer* **2008**, *99*, 1849−1858.

(6) Zhang, Q.; Fan, H.; Zou, Q.; Liu, H.; Wan, B.; Zhu, S.; Hu, Y.; Li, H.; Zhang, C.; Zhou, L.; Zhu, Q.; Xiao, K.; Zhang, J.; Zhan, P.; Lv, T.; Song, Y. TEAD4 exerts pro-metastatic effects and is negatively regulated by miR6839-3p in lung adenocarcinoma progression. *J. Cell. Mol. Med.* **2018**, *22*, 3560−3571.

(7) Liu, Y.; Wang, G.; Yang, Y.; Mei, Z.; Liang, Z.; Cui, A.; Wu, T.; Liu, C.-Y.; Cui, L. Increased TEAD4 expression and nuclear localization in colorectal cancer promote epithelial-mesenchymal transition and metastasis in a YAP-independent manner. *Oncogene* **2016**, *35*, 2789−2800.

(8) Zhou, Y.; Huang, T.; Zhang, J.; Wong, C. C.; Zhang, B.; Dong, Y.; Wu, F.; Tong, J. H. M.; Wu, W. K. K.; Cheng, A. S. L.; Yu, J.; Kang, W.; To, K. F. TEAD1/4 exerts oncogenic role and is negatively regulated by miR-4269 in gastric tumorigenesis. *Oncogene* **2017**, *36*, 6518−6530.

(9) Wang, C.; Nie, Z.; Zhou, Z.; Zhang, H.; Liu, R.; Wu, J.; Qin, J.; Ma, Y.; Chen, L.; Li, S.; Chen, W.; Li, F.; Shi, P.; Wu, Y.; Shen, J.; Chen, C. The interplay between TEAD4 and KLF5 promotes breast cancer partially through inhibiting the transcription of p27Kip1. *Oncotarget* **2015**, *6*, 17685−17697.

(10) Xu, M. Z.; Chan, S. W.; Liu, A. M.; Wong, K. F.; Fan, S. T.; Chen, J.; Poon, R. T.; Zender, L.; Lowe, S. W.; Hong, W.; Luk, J. M. AXL receptor kinase is a mediator of YAP-dependent oncogenic functions in hepatocellular carcinoma. *Oncogene* **2011**, *30*, 1229−1240.

(11) Barreto, S. C.; Ray, A.; Ag Edgar, P. Biological characteristics of CCN proteins in tumor development. *J. BUON* **2016**, *21*, 1359−1367.

(12) Zhao, B.; Ye, X.; Yu, J.; Li, L.; Li, W.; Li, S.; Yu, J.; Lin, J. D.; Wang, C.-Y.; Chinnaiyan, A. M.; Lai, Z.-C.; Guan, K.-L. TEAD mediates YAP-dependent gene induction and growth control. *Genes Dev.* **2008**, *22*, 1962−1971.

(13) Dong, J.; Feldmann, G.; Huang, J.; Wu, S.; Zhang, N.; Comerford, S. A.; Gayyed, M. F.; Anders, R. A.; Maitra, A.; Pan, D. Elucidation of a universal size-control mechanism in drosophila and mammals. *Cell* **2007**, *130*, 1120−1133.

(14) Ren, Y. R.; Chaerkady, R.; Hu, S.; Wan, J.; Qian, J.; Zhu, H.; Pandey, A.; Kern, S. E. Unbiased discovery of interactions at a control locus driving expression of the cancer-specific therapeutic and diagnostic target, mesothelin. *J. Proteome Res.* **2012**, *11*, 5301−5310.

(15) Chen, Z.; Friedrich, G. A.; Soriano, P. Transcriptional enhancer factor 1 disruption by a retroviral gene trap leads to heart defects and embryonic lethality in mice. *Genes Dev.* **1994**, *8*, 2293−2301.

(16) Kaneko, K. J.; Kohn, M. J.; Liu, C.; DePamphilis, M. L. Transcription factor TEAD2 is involved in neural tube closure. *Genesis* **2007**, *45*, 577−587.

(17) Nishioka, N.; Yamamoto, S.; Kiyonari, H.; Sato, H.; Sawada, A.; Ota, M.; Nakao, K.; Sasaki, H. TEAD4 is required for specification of trophectoderm in pre-implantation mouse embryos. *Mech. Dev.* **2008**, *125*, 270−283.

(18) Yagi, R.; Kohn, M. J.; Karavanova, I.; Kaneko, K. J.; Vullhorst, D.; DePamphilis, M. L.; Buonanno, A. Transcription factor TEAD4 specifies the trophectoderm lineage at the beginning of mammalian development. *Development* **2007**, *134*, 3827−3836.

(19) Juan, W.; Hong, W. Targeting the hippo signaling pathway for tissue regeneration and cancer therapy. *Genes* **2016**, *7*, 55.

(20) Santucci, M.; Vignudelli, T.; Ferrari, S.; Mor, M.; Scalvini, L.; Bolognesi, M. L.; Uliassi, E.; Costi, M. P. The hippo pathway and YAP/TAZ-TEAD protein-protein interaction as targets for regenerative medicine and cancer treatment. *J. Med. Chem.* **2015**, *58*, 4857−4873.

(21) Gibault, F.; Coevoet, M.; Sturbaut, M.; Farce, A.; Renault, N.; Allemand, F.; Guichou, J.-F.; Drucbert, A.-S.; Foulon, C.; Magnez, R.; Thuru, X.; Corvaisier, M.; Huet, G.; Chavatte, P.; Melnyk, P.; Bailly, F.; Cotelle, P. Toward the discovery of a novel class of YAP(-)TEAD interaction inhibitors by virtual screening approach targeting YAP(-)TEAD protein(-)protein interface. *Cancers* **2018**, *10*, 140.

(22) Gibault, F.; Sturbaut, M.; Bailly, F.; Melnyk, P.; Cotelle, P. Targeting transcriptional enhanced associate domains (TEADs). *J. Med. Chem.* **2018**, *61*, 5057−5072.

(23) Smith, S. A.; Sessions, R. B.; Shoemark, D. K.; Williams, C.; Ebrahimighaei, R.; McNeill, M. C.; Crump, M. P.; McKay, T. R.; Harris, G.; Newby, A. C.; Bond, M. Antiproliferative and antimigratory effects of a novel YAP-TEAD interaction inhibitor identified using in silico molecular docking. *J. Med. Chem.* **2019**, *62*, 1291−1305.

(24) Deng, X.; Fang, L. VGLL4 is a transcriptional cofactor acting as a novel tumor suppressor via interacting with TEADs. *Am. J. Cancer Res.* **2018**, *8*, 932−943.

(25) Pobbati, A. V.; Hong, W. Emerging roles of TEAD transcription factors and its coactivators in cancers. *Cancer Biol. Ther.* **2013**, *14*, 390−398.

(26) Chan, P.; Han, X.; Zheng, B.; DeRan, M.; Yu, J.; Jarugumilli, G. K.; Deng, H.; Pan, D.; Luo, X.; Wu, X. Autopalmitoylation of TEAD proteins regulates transcriptional output of the hippo pathway. *Nat. Chem. Biol.* **2016**, *12*, 282−289.

(27) Mesrouze, Y.; Meyerhofer, M.; Bokhovchuk, F.; Fontana, P.; Zimmermann, C.; Martin, T.; Delaunay, C.; Izaac, A.; Kallen, J.; Schmelzle, T.; Erdmann, D.; Chène, P. Effect of the acylation of TEAD4 on its interaction with co-activators YAP and TAZ. *Protein Sci.* **2017**, *26*, 2399−2409.

(28) Noland, C. L.; Gierke, S.; Schnier, P. D.; Murray, J.; Sandoval, W. N.; Sagolla, M.; Dey, A.; Hannoush, R. N.; Fairbrother, W. J.; Cunningham, C. N. Palmitoylation of TEAD transcription factors is required for their stability and function in hippo pathway signaling. *Structure* **2016**, *24*, 179−186.

(29) Kim, N.-G.; Gumbiner, B. M. Cell contact and Nf2/Merlin-dependent regulation of TEAD palmitoylation and activity. *Proc. Natl. Acad. Sci. U.S.A.* **2019**, *116*, 9877−9882.

(30) Pobbati, A. V.; Han, X.; Hung, A. W.; Weiguang, S.; Huda, N.; Chen, G.-Y.; Kang, C.; Chia, C. S. B.; Luo, X.; Hong, W.; Poulsen, A. Targeting the central pocket in human transcription factor TEAD as a potential cancer therapeutic strategy. *Structure* **2015**, *23*, 2076−2086.

(31) Bum-Erdene, K.; Zhou, D.; Gonzalez-Gutierrez, G.; Ghozayel, M. K.; Si, Y.; Xu, D.; Shannon, H. E.; Bailey, B. J.; Corson, T. W.; Pollok, K. E.; Wells, C. D.; Meroueh, S. O. Small-molecule covalent modification of conserved cysteine leads to allosteric inhibition of the TEAD-Yap protein-protein interaction. *Cell Chem. Biol.* **2019**, *26*, 378−389.

(32) Kaneda, A.; Seike, T.; Uemori, T.; Myojo, K.; Aida, K.; Danjo, T.; Nakajima, T.; Yamaguchi, D.; Hamada, T.; Tsuji, Y.; Hamaguchi, K.; Yasunaga, M.; Otsubo, N.; Onodera, H.; Nishiya, Y.; Suzuki, M.; Saito, J.; Ishii, T.; Nakai, R. Abstract 3086 Discovery of a first-in-class TEAD inhibitor which directly inhibits YAP/TAZ-TEAD protein-protein interaction and shows a potent anti-tumor effect in malignant pleural mMesothelioma. *Cancer Res.* **2019**, *79*, 3086.

https://dx.doi.org/10.1021/acs.jmedchem.0c01275
J. Med. Chem. 2020, 63, 11972−11989

(33) Lu, W.; Wang, J.; Li, Y.; Tao, H.; Xiong, H.; Lian, F.; Gao, J.; Ma, H.; Lu, T.; Zhang, D.; Ye, X.; Ding, H.; Yue, L.; Zhang, Y.; Tang, H.; Zhang, N.; Yang, Y.; Jiang, H.; Chen, K.; Zhou, B.; Luo, C. Discovery and biological evaluation of vinylsulfonamide derivatives as highly potent, covalent TEAD autopalmitoylation inhibitors. *Eur. J. Med. Chem.* **2019**, *184*, 111767.
(34) Li, Q.; Sun, Y.; Jarugumilli, G. K.; Liu, S.; Dang, K.; Cotton, J. L.; Xiol, J.; Chan, P. Y.; DeRan, M.; Ma, L.; Li, R.; Zhu, L. J.; Li, J. H.; Leiter, A. B.; Ip, Y. T.; Camargo, F. D.; Luo, X.; Johnson, R. L.; Wu, X.; Mao, J. Lats1/2 Sustain intestinal stem cells and Wnt activation through TEAD-dependent and independent transcription. *Cell Stem Cell* **2020**, *26*, 675−692.
(35) Kunig, V. B. K.; Potowski, M.; Akbarzadeh, M.; Klika Škopić, M.; Santos Smith, D.; Arendt, L.; Dormuth, I.; Adihou, H.; Andlovic, B.; Karatas, H.; Shaabani, S.; Zarganes-Tzitzikas, T.; Neochoritis, C. G.; Zhang, R.; Groves, M.; Guéret, S. M.; Ottmann, C.; Rahnenführer, J.; Fried, R.; Dömling, A.; Brunschweiger, A. TEAD-YAP interaction inhibitors and MDM2 binders from DNA-encoded indole-focused Ugi-peptidomimetics. *Angew. Chem., Int. Ed. Engl.* **2020**, *59*, DOI: 10.1002/anie.202006280
(36) Pobbati, A. V.; Mejuch, T.; Chakraborty, S.; Karatas, H.; Bharath, S. R.; Guéret, S. M.; Goy, P.-A.; Hahne, G.; Pahl, A.; Sievers, S.; Guccione, E.; Song, H.; Waldmann, H.; Hong, W. Identification of quinolinols as activators of TEAD-dependent transcription. *ACS Chem. Biol.* **2019**, *14*, 2909−2921.
(37) Holden, J. K.; Crawford, J. J.; Noland, C. L.; Schmidt, S.; Zbieg, J. R.; Lacap, J. A.; Zang, R.; Miller, G. M.; Zhang, Y.; Beroza, P.; Reja, R.; Lee, W.; Tom, J. Y. K.; Fong, R.; Steffek, M.; Clausen, S.; Hagenbeek, T. J.; Hu, T.; Zhou, Z.; Shen, H. C.; Cunningham, C. N. Small molecule dysregulation of TEAD lipidation induces a dominant-negative inhibition of hippo pathway signaling. *Cell Rep.* **2020**, *31*, 107809.
(38) Alexandrov, A. I.; Mileni, M.; Chien, E. Y. T.; Hanson, M. A.; Stevens, R. C. Microscale fluorescent thermal stability assay for membrane proteins. *Structure* **2008**, *16*, 351−359.
(39) Brune, M.; Corrie, J. E. T.; Webb, M. R. A fluorescent sensor of the phosphorylation state of nucleoside diphosphate kinase and its use to monitor nucleoside diphosphate concentrations in real time. *Biochemistry* **2001**, *40*, 5087−5094.
(40) Chung, C. C.; Ohwaki, K.; Schneeweis, J. E.; Stec, E.; Varnerin, J. P.; Goudreau, P. N.; Chang, A.; Cassaday, J.; Yang, L.; Yamakawa, T.; Kornienko, O.; Hodder, P.; Inglese, J.; Ferrer, M.; Strulovici, B.; Kusunoki, J.; Tota, M. R.; Takagi, T. A fluorescence-based thiol quantification assay for ultra-high-throughput screening for inhibitors of coenzyme A production. *Assay Drug Dev. Technol.* **2008**, *6*, 361−374.
(41) Goncalves, V.; Brannigan, J. A.; Thinon, E.; Olaleye, T. O.; Serwa, R.; Lanzarone, S.; Wilkinson, A. J.; Tate, E. W.; Leatherbarrow, R. J. A fluorescence-based assay for N-myristoyltransferase activity. *Anal. Biochem.* **2012**, *421*, 342−344.
(42) Smith, J. J.; Conrad, D. W.; Cuneo, M. J.; Hellinga, H. W. Orthogonal site-specific protein modification by engineering reversible thiol protection mechanisms. *Protein Sci.* **2005**, *14*, 64−73.
(43) Konopíková, M.; Uher, M.; Bransová, J.; Mastihuba, V.; Hudecová, D. Reaction of 5-hydroxy-2-hydroxymethyl-4H-pyran-4-one with aromatic aldehydes and amines (betti reaction). *Chem. Pap.* **1994**, *48*, 182−184.
(44) Burnett, C. L.; Bergfeld, W. F.; Belsito, D. V.; Hill, R. A.; Klaassen, C. D.; Liebler, D. C.; Marks, J. G., Jr.; Shank, R. C.; Slaga, T. J.; Snyder, P. W.; Andersen, F. A. Final report of the safety assessment of kojic acid as used in cosmetics. *Int. J. Toxicol.* **2010**, *29*, 244S−273S.
(45) Li, Y.; Liu, S.; Ng, E. Y.; Li, R.; Poulsen, A.; Hill, J.; Pobbati, A. V.; Hung, A. W.; Hong, W.; Keller, T. H.; Kang, C. Structural and ligand-binding analysis of the YAP-binding domain of transcription factor TEAD4. *Biochem. J.* **2018**, *475*, 2043−2055.
(46) Laraia, L.; Friese, A.; Corkery, D. P.; Konstantinidis, G.; Erwin, N.; Hofer, W.; Karatas, H.; Klewer, L.; Brockmeyer, A.; Metz, M.; Schölermann, B.; Dwivedi, M.; Li, L.; Rios-Munoz, P.; Köhn, M.; Winter, R.; Vetter, I. R.; Ziegler, S.; Janning, P.; Wu, Y.-W.; Waldmann, H. The cholesterol transfer protein GRAMD1A regulates autophagosome biogenesis. *Nat. Chem. Biol.* **2019**, *15*, 710−720.
(47) Medina-O'Donnell, M.; Rivas, F.; Reyes-Zurita, F. J.; Martinez, A.; Martin-Fonseca, S.; Garcia-Granados, A.; Ferrer-Martín, R. M.; Lupiañez, J. A.; Parra, A. Semi-synthesis and antiproliferative evaluation of PEGylated pentacyclic triterpenes. *Eur. J. Med. Chem.* **2016**, *118*, 64−78.

https://dx.doi.org/10.1021/acs.jmedchem.0c01275
J. Med. Chem. 2020, 63, 11972−11989